SEamless integratioN of efficient 6G WirelesS tEchnologies for Communication and Sensing

D4.5 Advanced Spectrum Management

April 2026

6G-SENSES project has received funding from the Smart Networks and Services Joint Undertaking (SNS JU) under the European Union's Horizon Europe research and innovation programme under Grant Agreement 101139282

Project Start Date: 2024-01-01 **Duration**: 30 months

Call: HORIZON-JU-SNS-2023 **Date of delivery**: 2026-04-17

Topic: HORIZON-JU-SNS-2023-STREAM-B-01-02 **Version**: 1.0

Dissemination Level: Public (PU)

Grant Agreement Number:	101139282
Project Name:	SEamless integratioN of efficient 6G WirelesS tEchnologies for Communication and Sensing
Project Acronym:	6G-SENSES
Document Number:	**D4.5**
Document Title:	Advanced Spectrum Management
Version:	1.0
Delivery Date:	2026-03-31 (**2026-04-17**)
Responsible:	TU Braunschweig (**TUBS**)
Editor(s):	Paul Nowitzki (**TUBS**)
Authors:	Paul Nowitzki, Thomas Kürner (**TUBS**), Muhammad Saadi (**NTU**), Khai Nguyen (**BR**), Jessica Sanson, Valerio Frascolla (**INT**).
Keywords:	6G, Wi-Fi, Spectrum Management, Interference Simulations, Interference Tests
Status:	Final
Dissemination Level	Public (PU)
Project URL:	https://www.6g-senses.eu

Revision History

Rev. N	Description	Author	Date
0.0	Draft Table of Contents (ToC)	Paul Nowitzki (**TUBS**)	2025-12-01
0.1	Added contributions to Sections 2-5 (Scenario 2)	Muhammad Saadi (**NTU**)	2026-01-22
0.2	Added contributions to Sections 1, 2 and 3, as well as partial contributions to Section 4	Paul Nowitzki (**TUBS**)	2026-02-26
0.3	Added interference ML models evaluation	Jessica Sanson (**INT**)	2026-03-05
0.4	Added remaining contributions to Section 4	Paul Nowitzki (**TUBS**)	2026-03-11
0.5	Added contributions to section 5.1	Khai Nguyen (**BR**)	2026-03-12
0.6	Added contributions to section 5.2	Thomas Kürner (**TUBS**)	2026-03-25
0.7	Final Review	Valerio Frascolla (**INT**), Ioanna Mesogiti (**OTE**)	2026-03-27
1.0	Last revision and submission of the document	Jesús Gutiérrez (**IHP**)	2026-04-17

Table of Contents

List of Figures

List of Tables

Executive Summary

The present deliverable **D4.5**, "Advanced Spectrum Management", investigates methods to enable efficient and interference-aware use of spectrum for emerging sixth Generation (6G) systems within the 6G-SENSES project. It focuses on three representative interference scenarios: cooperative integrated sensing and communication (ISAC) using monostatic Wi-Fi sensing, competitive spectrum sharing between Long-Term Evolution (LTE) and fifth Generation (5G) New Radio (NR), and coexistence between 5G NR-Unlicensed (NR-U) and Wi-Fi in the 6 GHz band and beyond. For each scenario, relevant frequency bands and interference control methods are identified, and their performance is evaluated through dedicated measurements and simulations.

In the ISAC scenario, the deliverable demonstrates that high-resolution Range-Doppler (RD) processing and range filtering on commercial 6 GHz Wi-Fi hardware enabled robust gesture recognition in interference-rich public environments, achieving accuracy above 90% while coexisting with regular Wi-Fi traffic.

To address and evaluate the application of spectrum sharing in (technologically) backwards compatible scenarios, the mobile network spectrum-sharing scenario is examined. In this case, co-primary shared access with spectrum pooling coordinated by a composite spectrum scheduler is shown to provide a flexible migration path from LTE to 5G, albeit with capacity losses under mixed-numerology operation due to inter-numerology interference.

For 5G NR-U/Wi-Fi coexistence in the 6 GHz band, Monte Carlo simulations reveal that static exclusion zones are effective mainly for indoor Wi-Fi deployments, while dense outdoor deployments require impractically large zones. Advanced beamforming techniques such as Minimum Variance Distortionless Response (MVDR) and narrow Gaussian beams can reduce interference by up to 7-13 dB in low- to medium-density cases but are insufficient as a stand-alone solution at high densities.

Building on these technical findings, the deliverable outlines integration strategies based on the Open-Radio Access Network (O-RAN) architecture, where the RAN Intelligent Controller (RIC) with rApps/xApps can realize dynamic spectrum sharing policies, numerology selection, and adaptive beam and exclusion-zone control in a closed loop. From a regulatory perspective, such dynamic spectrum sharing policies will become necessary aspects of future policies and recent developments by public agencies such as the Australian Communications and Media Authority (ACMA) and the UK OFCOM suggest that such policies are likely to be implemented in the future.

1 Introduction

Spectrum management is undergoing a structural crisis. For decades, regulatory practice has been built around static allocation of frequency bands to International Telecommunication Union - Radiocommunication sector (ITU-R) services and conservative, worst-case interference analyses based on fixed antenna patterns and maximum transmit powers. This paradigm was adequate for legacy wide-area broadcast and early cellular systems with relatively simple antenna technology and well-separated services. However, the emergence of highly dynamic, spatially selective radio technologies and multi-functional use of spectrum is rendering these traditional methods both overly pessimistic and practically infeasible. In particular, worst-case assumptions no longer capture the behaviour of beamformed links, Cell-Free massive MIMO (CF-mMIMO) architectures, or reconfigurable intelligent surfaces (RIS), all of which strongly depend on instantaneous channel conditions, network scheduling and spatial traffic distributions rather than on static link budgets.

The limits of the current regulatory methodology become even more evident with the advent of Integrated Sensing and Communication (ISAC) systems. In ISAC, multiple services – communication, radar-like sensing, and positioning – must coexist within the same bands and often even share the same waveforms and hardware. In frequency bands below 6 GHz, this raises the non-trivial question of coexistence between incumbent services and new ISAC deployments, but in the sub-THz regime shared spectrum access will be the default rather than the exception. Here, dense spatial reuse, highly directional links and fragile propagation conditions force regulators and operators to move beyond static worst-case interference envelopes toward context-aware, time-varying spectrum usage models. Without such a shift, either spectrum will be dramatically underutilised due to excessive protection margins, or harmful interference and regulatory non-compliance will become widespread.

6G-SENSES positions itself directly at this intersection of regulatory need and technological opportunity. The project designs and implements protocols for cellular/Wi-Fi traffic steering, offloading and backhauling across licensed and unlicensed spectrum, orchestrated by a centralised O-RAN controller in an RIS-enhanced CF-mMIMO environment. This architecture enables fine-grained control of spatial, spectral and temporal resource usage across heterogeneous networks, opening the door to dynamic spectrum management on very short time scales – down to minutes or even below. On top of this control fabric, 6G-SENSES realises an edge-based application layer that can observe, decide and act on spectrum utilisation in near-real time, thereby aligning operational decisions with regulatory constraints in a closed loop.

To achieve this vision, this deliverable first investigates dynamic methods for assessing interference compliance within existing and evolving regulatory frameworks. Instead of static worst-case evaluations, these methods exploit network state information, beam management and spatial traffic statistics to derive realistic interference envelopes that remain compatible with regulatory protection requirements. In parallel, new techniques for dynamic spectrum use in ISAC systems are explored, acknowledging that communication and sensing are still in their infancy as jointly managed spectrum users. These concepts are then realised prototypically in a sandbox environment, allowing safe experimentation with novel interference management, sharing policies and regulatory abstractions before wide-scale deployment.

1.1 State-of-the-Art Approaches to Spectrum Management

Modern spectrum management encompasses the coordinated set of administrative, legal, and technical measures required to ensure the efficient and interference-free use of the radio-frequency spectrum by all radiocommunication services. At the international level, the ITU provides the treaty-based framework for global spectrum coordination and regulation. The ITU Radio Regulations (RR), adopted and periodically revised by the World Radiocommunication Conference (WRC), define the frequency allocations (Article 5), regulatory conditions, and procedural obligations to be observed by national administrations. A central principle of the RR is that new uses must not cause harmful interference to existing services operating in accordance with these Regulations and recorded favourably in the Master International Frequency Register (MIFR) [1].

Between the ITU and national authorities, regional organizations such as the European Conference of Postal and Telecommunications Administrations (CEPT), the Inter-American Telecommunication Commission (CITEL), the Asia-Pacific Telecommunity (APT), and the Arab Council of Ministers for Telecommunication and Information play a critical coordinating role. Their objectives include the development of common positions for ITU deliberations, harmonization of national frequency allocations and certification procedures, and the facilitation of regional markets for radiocommunication equipment and services. In parallel, several specialized international organizations – active in sectors such as civil aviation, maritime operations, meteorology, broadcasting, space research, and radio astronomy – also contribute to global spectrum management and maintain close cooperation with the ITU [1].

This international framework reflects a balance between the sovereign right of states to regulate telecommunications and their collective responsibility to manage spectrum resources rationally. The ITU Constitution establishes guiding principles: avoiding harmful interference between national stations, enhancing the efficiency of spectrum and orbital resource usage, facilitating worldwide standardization and interoperability, and promoting international cooperation. While the RR affords significant flexibility – allowing multiple services per band and national choices regarding implementation – such flexibility can limit interoperability and economies of scale. Consequently, regional or global spectrum harmonization, notably for International Mobile Telecommunications (IMT) and related wireless technologies, remains essential for ensuring efficient use and facilitating the deployment of cross-border and global services. [1]

At the national level, the radio-frequency spectrum forms part of the public domain and is managed in the public interest under the authority of national legislation, regulations, and policy guidelines. Responsibilities usually rest with a specialized governmental department or independent regulatory authority. Core functions include maintaining a national frequency allocation table and register, coordinating stations for electromagnetic compatibility (EMC), implementing frequency assignments and licensing, and conducting monitoring and enforcement activities. Best regulatory practice emphasizes transparent and predictable decision-making, public consultation, and publication of allocation plans, with confidentiality applied only to cases involving national defence or security interests [1].

Recent spectrum management increasingly focuses on flexible, efficiency-oriented frameworks that can accommodate fast-evolving wireless ecosystems, where different communication technologies, e.g., mobile IMT (3G–6G), Wi-Fi, Internet of things (IoT), High-Altitude Platform Station (HAPS) and Non Geo-Stationary Orbit (NGSO) satellite constellations all compete for low-, mid- and high-band frequencies while simultaneously enabling new coverage and capacity models such as direct-to-device satellite and stratospheric platforms. Regulators are shifting from rigid, technology-specific allocations toward more dynamic tools. While keeping the basic framework intact, it is amended by concepts such as spectrum leasing and trading, shared access, as well as allocating bands for unlicensed access [2].

The Citizens Broadband Radio Service (CBRS) framework exemplifies an advanced model for dynamic spectrum management, enabling efficient and flexible use of mid-band spectrum via a coordinated sharing regime in the 3.5 GHz band. CBRS introduces a three-tier access hierarchy—Incumbent, Priority Access License (PAL), and General Authorized Access (GAA)—that allows different user categories to coexist while ensuring robust protection of higher-priority services. This arrangement is orchestrated by a cloud-based Spectrum Access System (SAS), which maintains a database of authorized radio systems, dynamically assigns frequencies and power levels, and proactively mitigates interference by relocating lower-tier users when incumbent activity is detected. By enabling localized, demand-driven access to spectrum for mobile operators, enterprises, and new verticals, CBRS demonstrates how algorithmic coordination and real-time spectrum assignments can enhance spectral efficiency, reduce underutilization, and support emerging 5G and private network deployments. Its principles and architecture are increasingly regarded as a reference for future European spectrum management approaches that aim to balance innovation, non-discriminatory access, and the protection of incumbent services [3].

In parallel, EU member state driven initiatives, such as Germany's 5G campus network approach, illustrate how localized licensing in harmonized mid-band spectrum can operationalize these principles in a European context. Since November 2019, the *Bundesnetzagentur* (*BNetzA*) has made 100 MHz in the 3.7–3.8 GHz band available for local 5G licenses on a site-specific, technology- and service-neutral basis, explicitly targeting non-public (private) networks for Industry 4.0, research, and other vertical sectors. Enterprises can apply for contiguous spectrum blocks (typically in 10 MHz steps) within a self-defined geographic area, with annual fees calculated according to bandwidth, license duration, and the size and location of the coverage area, thereby incentivizing efficient, needs-based use of the resource. BNetzA has also extended the local-licensing concept to 26 GHz, and by late 2024 had granted several hundred campus licenses in the 3.7–3.8 GHz band to actors such as manufacturers, Research and Development (R&D) facilities, and Information Technology (IT) service providers, underscoring strong industrial uptake of localized 5G spectrum [4].

Together, CBRS-style spectrum sharing and Germany's campus network model provide complementary reference cases for advanced spectrum management, combining dynamic coordination mechanisms with flexible local licensing to support private 5G and other innovative wireless applications.

1.2 Organisation of the document

This document is comprised of seven chapters. After the Executive Summary and the Introduction section:

- Chapter 2 describes the identified interference scenarios that are investigated in the following sections.
- Building on the interference scenarios defined in Chapter 2, Chapter 3, compiles the frequency bands as well as possible interference control mechanisms that are relevant to those scenarios and which are part of the simulation and test scenarios described in later sections.
- Chapter 4 is split into two subsections which describe the interference simulations and tests that were performed and their results, respectively.
- The possibilities to include the results from this deliverable in the 6G-SENSES RAN controller as well as future regulatory policies are discussed in Chapter 5.
- Chapter 6 concludes the deliverable, where a summary of the document and the main conclusions are put forward.

2 Identification of Interference Scenarios

This section introduces the different interference scenarios that are central to the advanced spectrum management concepts studied in this deliverable. It distinguishes between cooperative ISAC use cases, competitive spectrum sharing between cellular technologies, and coexistence between cellular and Wi-Fi systems in the 6 GHz band and beyond. These scenarios form the basis for the subsequent analysis of relevant frequency bands, interference control methods, and the simulations and tests presented in later sections.

2.1 Interference between the wireless system and another service used in ISAC (cooperative scenario)

The work described in this section evaluates a cooperative ISAC scenario focusing on gesture recognition using a commercial off-the-shelf (COTS) laptop. As indicated in Figure 2-1, the system operates with a monostatic full-duplex sensing pipeline, which, unlike traditional bistatic systems that rely on separated transmitter and receiver pairs, captures gestures on a single device by sharing the Local Oscillator (LO) and Baseband processing between the Transmit (Tx) and Receive (Rx) chains. In this setup, the system simultaneously maintains normal Wi-Fi communication and Internet connectivity with no Network Interface Card (NIC) modification. The primary interference challenge investigated in this scenario arises in uncontrolled, crowded public environments characterized by dense foot traffic and active monostatic Wi-Fi devices.

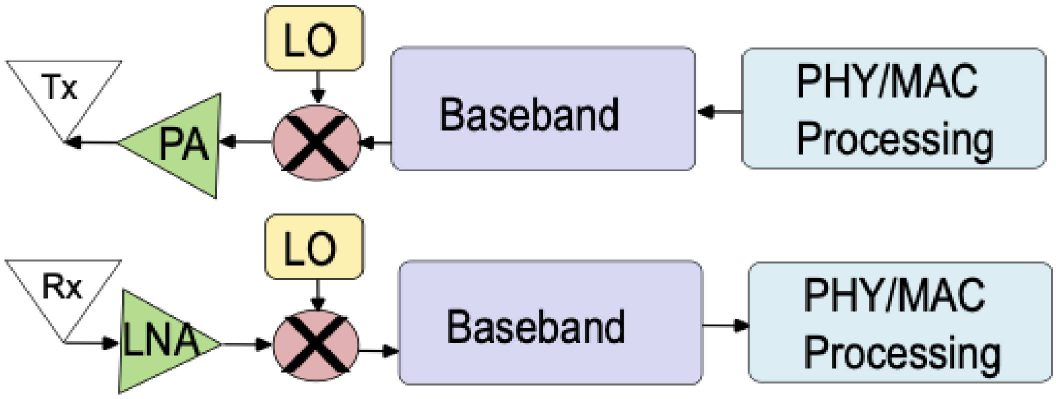

Figure 2-1 Monostatic Wi-Fi sensing mode utilizes a shared LO and Baseband processor on a single device.

2.2 Interference between the wireless system and another service (competitive scenario)

The 5G network is a multi-use-case networking environment that allows the coexistence of diverse services, different deployment options, multiple spectral bands and different resource provisioning approaches. The goal of 5G networks is to provide significant enhancements over the legacy LTE networks. To facilitate smooth transition from LTE to 5G-NR, several techniques that, at first, enable coexistence of LTE and 5G-NR have been explored. Among the possible migration options, spectrum sharing has attracted significant interest due to its comparative spectral efficiency, coverage, capacity (though limited), cost and time advantages. As for spectrum sharing, it allows incumbents and other new networks to simultaneously share the same spectral resources. For example, in the case of LTE and 5G-NR coexistence, spectrum sharing allows an existing LTE carrier to be used to operate 5G-NR and LTE simultaneously. Under the limited spectral resources, spectrum sharing facilitates smooth evolution from LTE to 5G using low frequency bands to achieve wide coverage for 5G network. It also offers low total cost of ownership to launch 5G in bands currently used for LTE, thus enabling timely nationwide 5G coverage. Figure 2-2 shows an exemplary multi-tier and multi-Radio Access Technology (RAT) system architecture.

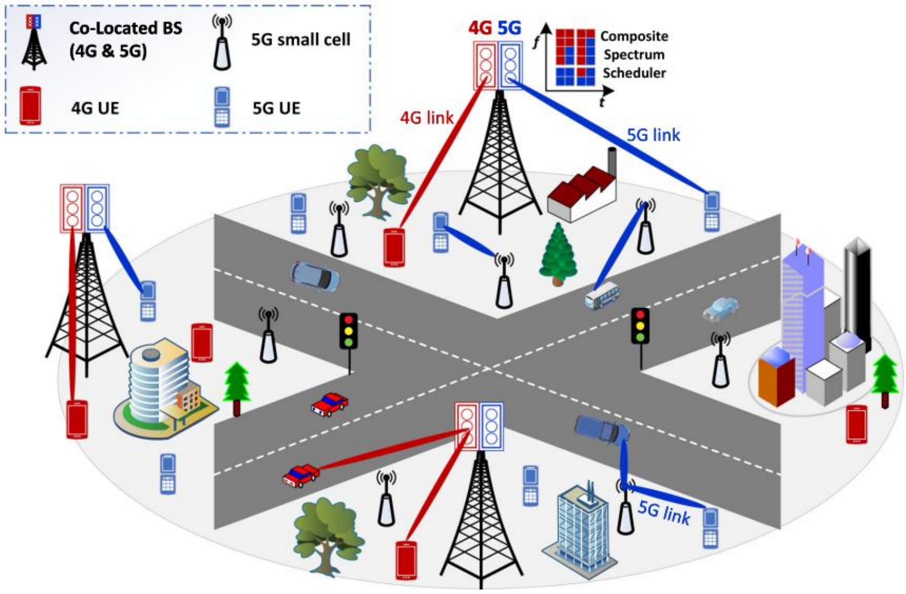

Figure 2-2 Multi-tier (macro and small cells) and multi-RAT (LTE and 5G-NR) system architecture

With respect to architecture, we focus on spectrum sharing based on the co-primary shared access. This involves either one mobile network operator (MNO) with two coexisting RATs (LTE and 5G-NR) or two MNOs with one MNO operating LTE and the other MNO operating 5G-NR. Beyond the spectrum sharing, this co-primary shared access application scenario can further be seen as passive sharing with respect to the network infrastructure. Here, the co-located Base Stations (BSs) share the same mast, cooling equipment and power supply, but not antenna or transmission equipment. As a sub-class of the considered co-primary shared access, we further focus on the spectrum pooling approach. By spectrum pooling, both the LTE and 5G-NR RATs have equal access to the spectrum, with neither any priority nor any opportunistic access via spectrum sensing. Here, only a super resource scheduler (herein referred to as composite spectrum scheduler) is required for coordinated resource allocation.

Spectrum sharing allows the allocation of dedicated carriers in the same frequency band to different standards (e.g., both LTE and 5G-NR sharing the same 20 MHz LTE bandwidth). It is a transition phase while migrating from the legacy LTE to the target 5G-NR network that provides improved capability and flexibility. Spectrum sharing requires the use of the so-called super resource scheduler or spectrum broker to coordinate resource allocation between the two coexisting RATs. The composite spectrum scheduler is composed of two different schedulers (i.e., the LTE and 5G-NR schedulers) that are synchronized for resource allocation. The coordination ensures that if a Resource Block (RB) is allocated by the LTE scheduler, that RB becomes unavailable for scheduling at the 5G scheduler, and vice-versa. For spectrum sharing, some RBs are dedicated to the coordination control thereby incurring additional signalling overhead and reducing the spectral resources available for data transmission. The LTE and 5G-NR schedulers coordinate with each other through the instantaneous exchange of traffic or RB allocation status.

We employ the dynamic user parameter for scheduling where the number of users in each RAT determines the share of spectrum for the RAT. This parameter can be chosen at the start of simulation and remains constant throughout (static spectrum sharing), or changes dynamically from one Transmission Time Interval (TTI) chunk to another for the dynamic spectrum sharing scenario. Thus, the policy is co-primary shared access with spectrum pooling, implemented through a composite spectrum scheduler and a dynamic user-based spectrum allocation policy, with Round Robin scheduling at the RAT level. Spectrum evolution and scheduler are shown in Figure 2-3.

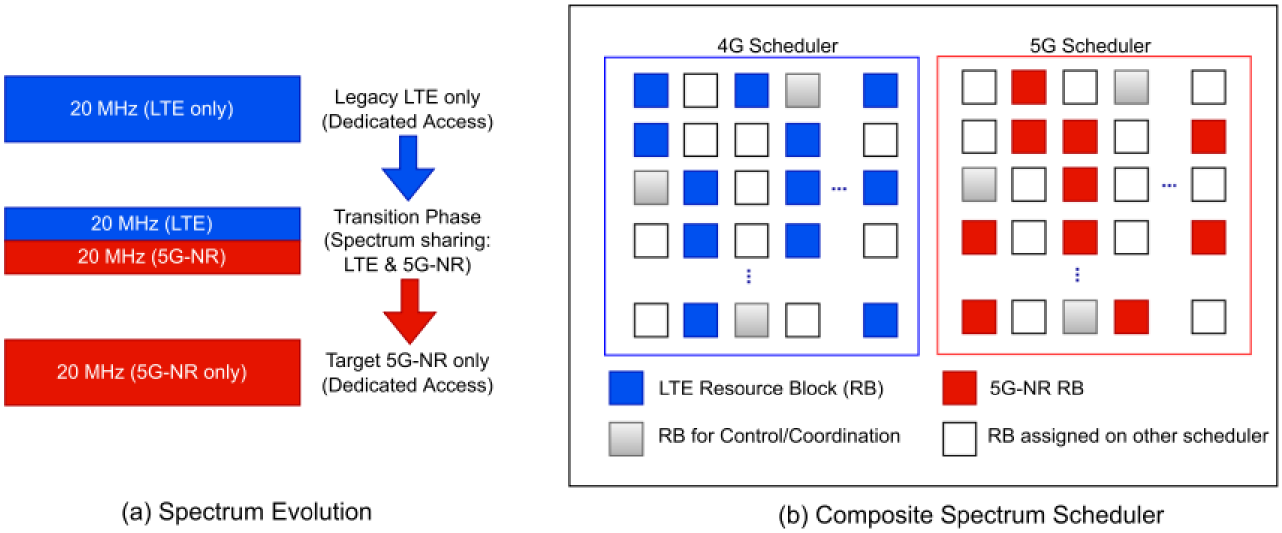

Figure 2-3 Spectrum sharing evolution and composite spectrum scheduler

Although the spectrum sharing technology has the aforementioned advantages, it introduces a lot of interference between the different RATs which typically affects the network performance with respect to User Equipment (UE) throughput and network capacity. This is due to the possible misalignment between LTE and 5G-NR RB scheduling. Another challenge in using spectrum sharing concerns how to ensure high network flexibility that accommodates the differences in scheduling time, frame structure and other components of the coexisting RATs. Using LTE and 5G-NR spectrum sharing as an example, the minimum scheduling time granularity of the two technologies sharing the spectrum could differ, since the 5G-NR RAT uses variable numerology. Unlike the fixed numerology of LTE, 5G-NR can adapt the frame size and subcarrier spacing based on the selected numerology. Supporting heterogeneous 5G services in spectrum sharing networks leads to mixed numerology profiles where LTE and 5G-NR use different numerologies. However, this mixed numerology profile leads to a number of challenges in coexisting LTE and 5G-NR networks exploiting spectrum sharing. Some of the challenges include: inter-numerology interference (INI), low spectral efficiency due to increased spectrum overhead, and more complex resource scheduling with high signalling overhead. The difference in numerology between coexisting RATs that leads to INI is typically mitigated using flexible and intelligent scheduling of RBs. Furthermore, the minimum time interval for spectrum sharing configuration change is typically chosen as 1 ms being the coarser granularity of the LTE and 5G-NR coexisting RATs. Dynamic Spectrum sharing (DSS) addresses the limitations of static spectrum sharing, though at the expense of higher RB and signalling overhead. Thus, the interference scenario is explicitly modelled as inter-numerology interference, arising from non-orthogonal frame structures when LTE and 5G-NR use different numerologies. The mitigation approach is coordinated RB scheduling via the composite spectrum scheduler and careful selection of scheduling granularity, while the performance impact of residual INI is quantified in capacity results.

2.3 Interference between the cellular system and the Wi-Fi system at 6 GHz and beyond

The accelerating demand for high-throughput wireless communication has led to the full allocation of the sub-6 GHz spectrum, prompting the industry to explore the 6 GHz range (5.925 - 7.125 GHz) as a critical band for next-generation systems. This frequency range offers several advantages, including wide bandwidth availability, flexibility for unlicensed operation, and relatively low congestion compared to legacy bands. Wi-Fi technologies under the IEEE 802.11ax (Wi-Fi 6E) and 802.11be (Wi-Fi 7) standards are used in this band, with contiguous and non-contiguous channels up to 320 MHz to support high data rates and multi-link operation. In parallel, IMT initiatives have identified the same spectrum for 5G NR-U operation, leading to a shared-spectrum scenario between Wi-Fi and cellular systems [5].

This co-band utilization introduces new interference and coexistence challenges. In dense urban environments, both technologies may compete for spectrum access, causing potential degradation in throughput, latency, and Quality of Service (QoS). The situation is further complicated by the heterogeneous deployment characteristics of each system: Wi-Fi primarily operates indoors at lower power levels, while 5G NR-U BSs can serve larger outdoor areas, possibly leading to cross-system interference where coverage overlaps. To mitigate interference, regulatory frameworks such as the Federal Communications Commission (FCC) Automated Frequency Coordination (AFC) system govern standard-power unlicensed operation within sub-bands like U-NII-7 (6.525 - 6.875 GHz). These AFC systems dynamically assign frequencies and power limits based on geolocation, ensuring protection for incumbent fixed services and satellite links. However, their effectiveness in dense deployments involving numerous Wi-Fi Access Points (APs) and 5G NR-U nodes remains under investigation [5].

Recent studies provide mixed insights. Simulations show that Wi-Fi devices can coexist with incumbents under low-density conditions, but large-scale measurements using smartphones and drones reveal that dense Wi-Fi 6E deployments can measurably elevate outdoor signal levels. Further experimental analyses assess aggregate interference from both Wi-Fi and 5G NR-U, suggesting coexistence may remain feasible if managed carefully through adaptive exclusion zones, e.g., geofenced areas where one system restricts transmission to reduce aggregate interference [5].

In the 6 GHz band, particularly the U-NII-7 range allocated for standard-power unlicensed operation, coexistence between 5G NR-U BSs and Wi-Fi 6E/7 APs under co-channel operation creates several distinct interference scenarios that depend strongly on deployment type, spatial configuration, and propagation conditions. These scenarios are driven by mutual interference in both directions, Wi-Fi towards cellular (uplink interference at the IMT/NR-U BS) and cellular towards Wi-Fi (downlink interference at Wi-Fi user devices), and are further shaped by building penetration losses [5].

Therefore, section investigates two key scenarios using simulations to evaluate the influence of different interference control methods described in Section 3.2. The first key scenario concerns aggregate interference produced by many Wi-Fi devices operating co-channel with a 5G NR-U BS in the upper 6 GHz band, where both systems share the same carrier frequency (e.g., 6.775 GHz) and overlapping coverage in urban environments of varying density. Here, NR-U BSs act as the victim receivers while Wi-Fi APs and stations are the interfering transmitters, with aggregate interference modelled as the sum of contributions from all simultaneously active Wi-Fi devices within the considered area, including those outside any exclusion zone around the BS [5]. The reciprocal scenario considers interference at Wi-Fi receivers (typically client devices) caused by co-channel transmissions from a nearby 5G NR-U BS, which in this context acts as the dominant single interferer rather than an aggregate source. Wi-Fi devices experience harmful interference when the NR-U signal at their receiver input exceeds the interference margin implied by the required signal-to-interference-plus-noise ratio for the selected modulation and coding scheme and bandwidth [5].

3 Relevant Frequency Bands and Interference Control Methods

This chapter identifies the key frequency bands utilized in the three interference scenarios described in Section 2 and examines the interference control mechanisms relevant to each scenario. The analysis focuses primarily on the 6 GHz band, where Wi-Fi 6E/7 and 5G NR-U systems operate in shared spectrum, as well as the sub-6 GHz range (2.1 GHz) for LTE and 5G-NR coexistence. For each scenario, specific interference mitigation techniques are outlined, including range filtering for Wi-Fi sensing, coordinated scheduling for spectrum sharing, and spatial techniques such as exclusion zones and beamforming for cellular-Wi-Fi coexistence.

3.1 Identification of Relevant Frequency Bands

For the Wi-Fi monostatic sensing scenario defined in section 2.1, operations are conducted in the 6 GHz band. Specifically, the system utilizes channel 79, which corresponds to a centre frequency of 6.345 GHz, operating with a bandwidth of 160 MHz and 512 subcarriers.

In this specific frequency range, the system shares the spectrum with several other commercial technologies, leading to potential co-channel interference. Primary sources of interference evaluated in this context include:

- **Wi-Fi 6E and Wi-Fi 7:** Devices operating under the IEEE 802.11ax (Wi-Fi 6E) and 802.11be (Wi-Fi 7) standards utilize this same spectrum. Because these standards support wide contiguous and non-contiguous channels up to 320 MHz, other nearby APs and client devices can create significant aggregate interference.
- **Cellular Systems (5G NR-U):** IMT initiatives have identified the 6 GHz range for 5G NR-U operation, creating a shared-spectrum scenario where 5G NR-U BSs and UE can cause cross-system interference.

The work described in Section 2.2 evaluates LTE and 5G-NR spectrum sharing in the sub-6 GHz range, using a carrier frequency of 2.1 GHz. A total bandwidth of 20 MHz is considered to represent typical mid-band spectrum used for legacy LTE and early 5G deployments.

Section 2.3 considers different interference control mechanisms for Wi-Fi and 5G NR-U devices in co-channel operation. As previously stated, the 6 GHz band is a key frequency range for this scenario, especially considering that the U-NII-7 sub-band is allocated for standard-power unlicensed operation. Therefore, subsequent evaluations and simulations are carried out in the 6 GHz band, using a carrier frequency of 6.775 GHz which is located both in the centre region of the 6 GHz band as a whole and inside the U-NII-7 sub-band.

3.2 Identification of Interference Control Methods

To address the interference challenges identified for the scenario described in Section 2.1, the primary control method utilized is range filtering applied to RD maps. By utilizing spatial range information, the system can isolate the intended gesture occurring in the foreground, e.g., at 20 cm.

Furthermore, transforming the channel state information across multiple subcarriers into the range domain provides a significant coherent processing gain. For example, operating on a 160 MHz bandwidth with 512 subcarriers yields a Signal to Noise Ratio (SNR) processing gain of approximately 27.1 dB. This processing gain inherently attenuates non-coherent interference signals across space, significantly enhancing the robustness of the system against ambient wireless traffic. Additionally, hardware-level interference control is achieved through an algorithmic synchronization phase that performs delay and phase alignment, alongside self-interference cancellation to remove Tx/Rx coupling.

Interference management in LTE and 5G-NR spectrum sharing described in Scenario 2 (Section 2.2) primarily focuses on addressing inter-numerology interference arising from differences in frame structure, subcarrier spacing, and scheduling granularity between the two RATs. Mixed numerology operation, where LTE uses a fixed numerology and 5G-NR employs flexible numerologies, introduces non-orthogonal RBs that can generate INI. This interference is typically controlled through flexible and intelligent RB scheduling, including INI-aware scheduling and QoS-aware and channel-aware resource allocation frameworks designed for mixed numerology systems. Standardized DSS mechanisms defined in 3GPP Releases 15–17, such as Multicast-Broadcast Single-Frequency Network (MBSFN)-based, mini-slot-based, and rate-matching-based, provide practical interference avoidance procedures for LTE–NR coexistence. In coordinated spectrum sharing, a composite spectrum scheduler synchronizes LTE and 5G-NR schedulers to ensure that RBs assigned to one technology are not simultaneously assigned to the other, thereby preventing direct RB collisions. Additionally, spectrum sharing configuration updates are aligned to a common scheduling time granularity to accommodate differences in LTE and 5G-NR transmission time intervals. Together, coordinated scheduling, standardized DSS signalling structures, and numerology-aware resource allocation form the principal interference control mechanisms applied in LTE–5G spectrum sharing systems.

The first mitigation concept for interference Scenario 3 considered in Section 2.3 is the implementation of geolocation-based exclusion zones around sensitive receivers, a regulatory tool already used to protect fixed services and being extended in the 6 GHz band via AFC systems. In the studied 5G NR-U/Wi-Fi coexistence scenarios, exclusion zones are applied around NR-U BSs to prevent Wi-Fi deployments within a certain radius, with the radius treated as a design variable; this directly reduces the number and proximity of interferers and is particularly effective for indoor Wi-Fi deployments where additional propagation losses already exist. The results indicate that, for indoor Wi-Fi, relatively modest exclusion radii can enable safe co-channel operation, whereas outdoor Wi-Fi may require very large exclusion zones, which reduces spectrum utilization and may be impractical in dense urban environments, suggesting that exclusion zones alone are insufficient as a universal coexistence mechanism. AFC concepts proposed for 6 GHz, e.g., by Qualcomm and Intel, envision database-driven, location-aware control of power, frequency, and potentially exclusion radii to protect incumbents; extending such systems to also account for NR-U/Wi-Fi coexistence could support dynamic, context-dependent interference management beyond static exclusion zone design. This points to a two-tier interference management approach in the 6 GHz and higher bands, where simple geolocation-based exclusion zones provide a baseline in lower-interference, predominantly indoor scenarios, while more sophisticated DSS and coordination, e.g., adaptive channel selection, power control, or beamforming, becomes necessary in dense outdoor or mixed deployments to adequately manage mutual interference between cellular and Wi-Fi systems.

In addition to spatial separation by exclusion zones, advanced beamforming at 5G NR-U BSs are investigated as another concept to mitigate interference in the coexistence scenario for Wi-Fi and 5G NR-U. In particular, there are two methods that have been successfully used in similar situations.

The Minimum-Variance Distortionless Response (MVDR) algorithm is a procedure to calculate the beamforming weights for a uniform linear array (ULA) of antennas such that the direction of the beam can be varied arbitrarily. The key feature of MVDR is that it allows for introducing a theoretically unlimited number of nulls in the beamforming diagram at any desired angle which enables the attenuation of specific sources of interference. This approach has been used in combination with others in [6] to implement a prototypical 5G NR BS that was able to improve energy performance by 50% in a small-scale test setup using one BS and two UE each, for 5G and Wi-Fi, in co-channel operation at a carrier frequency of 2550 MHz. We adapt the MVDR algorithm to a sandbox environment to evaluate its performance in a larger-scale simulation.

A second approach to beamforming is centred around Gaussian beams as a means to simulate beams in a mathematically controlled way that directly parameterizes beam width, divergence, and on-axis power density. Classical Gaussian beam theory models the complex field envelope of a quasi-collimated beam as a solution of the paraxial wave equation, characterized by a beam waist w_0, a position-dependent beam radius

$w(z)$, and a radius of curvature $R(z)$. For a symmetric fundamental mode, the transverse field and power density follow $E(r,z) \propto exp\left(\frac{-r^2}{w^2(z)}\right)$d $P(r,z) \propto exp\left(\frac{-2r^2}{w^2(z)}\right)$, respectively. These parameters are linked via compact formulas such as $w(z) = w_0\sqrt{1+\left(\frac{z}{z_c}\right)^2}$ and $R(z) = z\left(1+\left(\frac{z}{z_c}\right)^2\right)$, where the confocal distance $z_c = \frac{\pi w_0^2}{\lambda}$ (Rayleigh range) defines the transition between a near-field region with almost constant beam width and a far-field region with approximately linear angular spreading [7].

For 5G NR-U and Wi-Fi antenna arrays operating in the 6 GHz band and above, the results from this simulation approach can be interpreted as a design framework for Gaussian-like array patterns, where the discrete beamforming weights are chosen such that the far-field envelope approximates a fundamental Gaussian mode with a prescribed waist at or near the array aperture, thus fixing the far-field beamwidth and divergence angle.

4 Simulation and Test Setups and Results of Interference Scenarios

This chapter presents the comprehensive simulation frameworks and experimental test configurations developed to evaluate the three interference scenarios identified in Chapter 2, along with their corresponding results. The methodologies range from real-world gesture recognition tests using commercial Wi-Fi hardware in public environments, to Monte Carlo simulations modelling aggregate interference between 5G NR-U BSs and Wi-Fi devices at varying deployment densities. Each subsection details the specific parameters, propagation models, and performance metrics used to quantify interference levels and assess the effectiveness of different mitigation strategies.

We first start describing the detailed experimental and simulation environments established for each of the three interference scenarios. **Scenario 1** employs a real-world test setup using a commercial laptop with monostatic Wi-Fi sensing in controlled and public environments to evaluate gesture recognition under interference conditions. Scenarios 2 and 3 utilize sophisticated simulation frameworks: **Scenario 2** models LTE and 5G-NR spectrum sharing in a multi-cell hexagonal deployment with varying user distributions and numerology profiles, while **Scenario 3** implements Monte Carlo simulations to assess co-channel interference between 5G NR-U and Wi-Fi systems in the 6 GHz band under different deployment densities and mitigation strategies.

Finally, we present the quantitative findings from the interference experiments and simulations described in section **Error! Reference source not found.**. Results demonstrate that range filtering enables robust Wi-Fi gesture recognition with 90.54% accuracy even in densely populated public spaces, while mixed-numerology operation in LTE/5G-NR spectrum sharing introduces measurable capacity degradation due to inter-numerology interference. For 6 GHz coexistence, the analysis reveals that exclusion zones alone are promising for indoor Wi-Fi deployments, but insufficient for outdoor Wi-Fi deployments, whereas advanced beamforming techniques (MVDR and narrow Gaussian beams) can reduce interference by 7-13 dB in lower-density scenarios, though their effectiveness diminishes rapidly as deployment density increases.

4.1 Scenario 1

4.1.1 Description and test setup

Building upon the cooperative ISAC scenario defined in Section 2.1, the interference test setup evaluates monostatic Wi-Fi sensing using a single unmodified commercial laptop (Lenovo ThinkPad L14) equipped with an Intel Wi-Fi 6E AX211 NIC. The system operates on channel 79 (6.345 GHz centre frequency) with a bandwidth of 160 MHz, 512 subcarriers, and a frame rate of 40 Hz. This configuration provides high-resolution spatial awareness, achieving RD resolutions of 0.93 cm and 0.03 m/s, respectively.

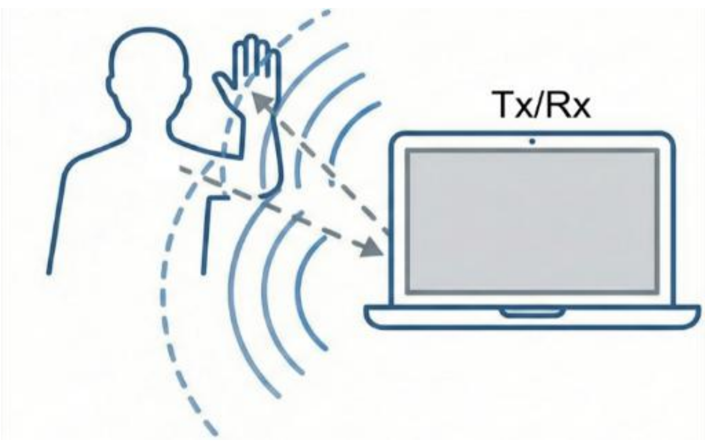

Figure 4-1 Wi-Fi monostatic sensing setup for gesture recognition

To ensure a robust evaluation of interference and generalization, a comprehensive dataset of 191,000 frame samples was collected from five distinct users. The users were instructed to perform five common gestures: (1) Push & Pull, (2) Slide, (3) Up-Down, (4) Double Pulse, and (5) Double Rotate, as simplified in Figure 4-1. Data collection spanned multiple environments to capture varying levels of multipath and interference:

- **Controlled Environments:** Baseline training data was collected in two indoor locations, i.e., a furnished office room and an open meeting room, yielding 720 total gesture instances.
- **Public Space (Interference Environment):** To assess real-world robustness, a third unseen public space location (a cafe) was used exclusively as an out-of-domain test set. This environment was characterized by dense foot traffic and active monostatic Wi-Fi devices. During these tests, at least three individuals were seated less than 1.5 m from the experiment, around ten people were within 5 m, and multiple people frequently walked within 2 m of the experimental area, creating a highly dynamic interference scenario.

4.1.2 Simulation and test results

The test results for the Wi-Fi sensing setup described in section 4.1 provide a comprehensive benchmark of deep learning models and demonstrate the significant advantage of utilizing range information for interference mitigation. Several neural network architectures were evaluated (see Table 4-1), including 3D Convolutional Neural Networks (CNNs), ResNet3D variants, Video Transformers (ViViT, TimeSformer), and hybrid CNN - Recurrent Neural Networks (RNN) / Gated Recurrent Unit (GRU) / Long-Short Term Memory (LSTM) models.

In the challenging public space environment, relying on Doppler processing alone (which mimics bistatic sensing by taking the mean over all subcarriers) resulted in severe visible signal degradation due to interference from bystanders. However, applying range filtering to exclude targets beyond 1 m robustly suppressed this background noise and isolated the intended gestures.

Thanks to this interference attenuation, the temporal CNN-GRU model maintained a highly resilient recognition accuracy of 90.54% in the public space. The additional range dimension was crucial for supporting generalization in this complex environment. In contrast, architectures lacking explicit mechanisms for temporal modelling, such as ResNet3D and 3D CNN, faced significant difficulty distinguishing the intended gesture from residual background noise and wireless interference. Consequently, these 3D convolutional models experienced a performance degradation in accuracy under the same uncontrolled conditions.

Table 4-1 Performance comparison – Wi-Fi gesture recognition on interference scenarios

Model	Public Space Acc. (%)	Public Space F1 (%)
3D CNN	60.81	63.12
CNN-GRU	90.54	87.77
CNN-LSTM	83.78	82.89
CNN-RNN	79.73	76.79
ResNet3D-10	79.73	77.63
ResNet3D-18	82.43	82.27
ResNet3D-50	79.73	80.76
TimeSformer	75.68	75.67
ViViT	79.73	81.01

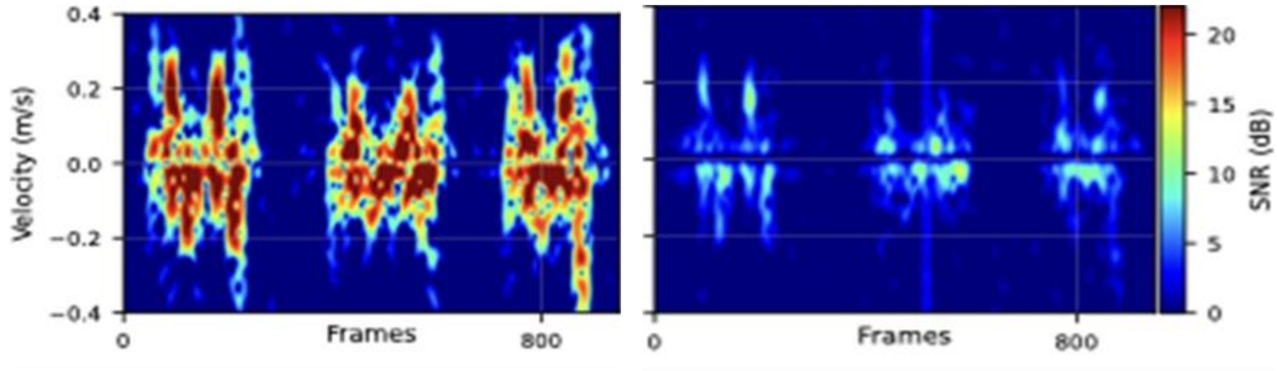

Figure 4-2 Spectrograms for three consecutive rotate gestures, comparing effect of using range to filter out background interference on Doppler information. Left: With range filtering (>1m) and right: Without range filtering (all subcarriers).

In Figure 4-2 we compare the velocity spectrograms of consecutive rotate gestures under public space environment affect by interference signals, with and without using range information to filter out background motion. Using range information to filter out distant gates (> 1 m) significantly improves the SNR. In the public space, using Doppler processing only (based on bistatic sensing/mean over all subcarriers) results in visible degradation due to interference from bystanders. In contrast, range filtering robustly suppresses background noise and enables reliable gesture detection, underscoring its importance for practical Wi-Fi sensing applications in the real world.

4.2 Scenario 2

4.2.1 Description and test setup

The simulation environment in Scenario 2 is based on two deployment layouts representing baseline and coexistence scenarios. Figure 4-3 (a) illustrates the dedicated-access layout, where either all BSs operate LTE or all operate 5G-NR, using exclusive spectrum access. The layout consists of a hexagonal grid of seven sites with tri-sectored macrocells, amounting to 21 BS sectors, serving 200 UE randomly distributed over a 2 × 2 km² area. Figure 4-3 (b) extends this setup to the spectrum sharing scenario by co-locating a 5G-NR BS sector at each LTE sector, resulting in 21 LTE and 21 5G-NR sectors operating in the same geographical area. In this coexistence layout, LTE BSs serve LTE users and 5G-NR BSs serve 5G users, while both RATs share the same frequency band under coordinated spectrum allocation.

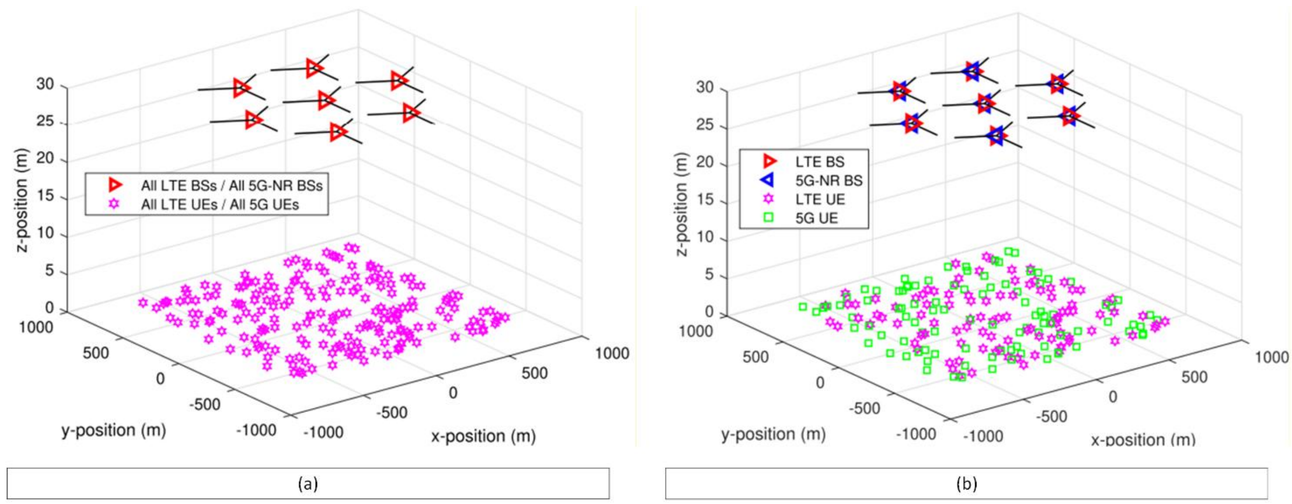

Figure 4-3 (a). LTE only or 5G-NR only network showing dedicated access. (b). LTE and 5G-NR co-existence network showing spectrum sharing

To evaluate different coexistence configurations, multiple LTE-to-5G user and spectrum sharing ratios are defined, as illustrated in Figure 4-4. 200 users are maintained in the network, with user distributions ranging from LTE-dominant to 5G-dominant scenarios. Correspondingly, the available 20 MHz bandwidth is partitioned into different LTE-to-5G spectrum shares, representing early, intermediate, and advanced stages of 5G adoption. These combinations provide a structured set of test cases for assessing the impact of varying user populations and spectrum allocations in static spectrum sharing conditions.

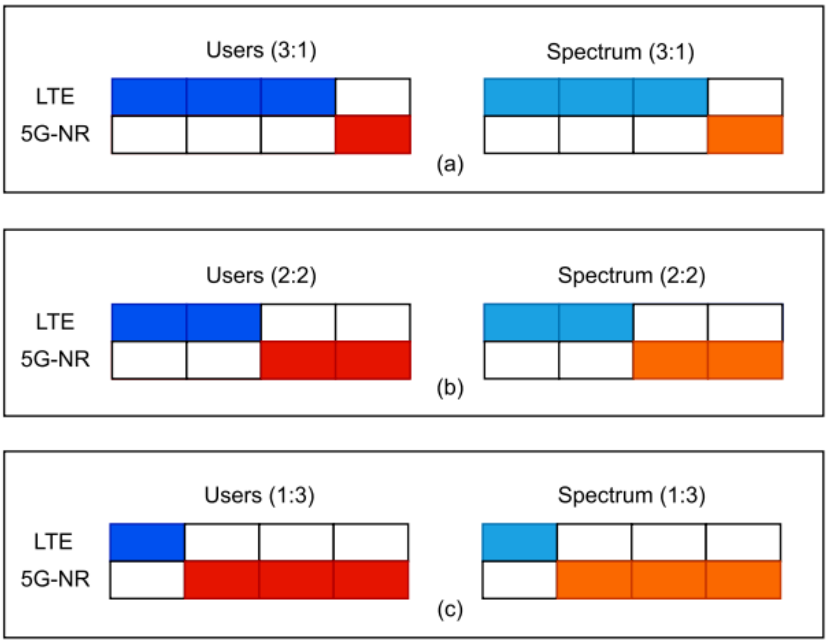

Figure 4-4 Spectrum sharing and user ratio

Table 4-2 summarizes the used baseline parameters.

Table 4-2 Baseline parameters

Parameter	LTE and 5G-NR
Carrier frequency [fc]	2.1 GHz
Bandwidth	20 MHz
BS sector layout	Tri-sectored macrocells
BS inter-site distance [ISD]	500 m
BS transmit power	46 dBm
BS height	30 m
UE height	1.5 m
Macroscopic fading	3GPP TR 36.873
Small-scale fading	Ped-A fast-fading model
No. of TX & RX antennas	4×4
MIMO transmission mode	CLSM
Waveform	OFDM
Numerology index (μ)	0
Subcarrier spacing	15 kHz
Scheduler	Round Robin
Traffic	Full Buffer

4.2.2 Simulation and test results

Impact of user and spectrum sharing ratios on total network capacity

Prior to examining numerology effects, the impact of spectrum sharing on overall network capacity is assessed by comparing three configurations: LTE-only (dedicated access baseline), LTE–5G-NR spectrum sharing (coexistence), and 5G-NR-only (dedicated access target). Under 4×4 MIMO and equal user and spectrum sharing ratios (100 LTE UEs: 100 5G-NR UEs; 10 MHz: 10 MHz), the network capacities are 551.47, 670.62, and 990.67 Mbits/s for the LTE-only, spectrum sharing, and 5G-NR-only configurations, respectively. These results demonstrate that while spectrum sharing achieves a moderate capacity gain over the LTE-only network, it falls substantially short of the 5G-NR-only network capacity. The limited gain in spectrum sharing arises from the trade-off between the higher modulation and coding scheme (MCS) advantage of the 5G-NR tier (QPSK–256QAM versus LTE's QPSK–64QAM) and the overhead incurred by the composite spectrum scheduler, which reserves a portion of resource blocks for inter-RAT coordination and control signalling. Furthermore, the constituent LTE and 5G-NR parts within the spectrum sharing network individually achieve lower capacities than their dedicated-access counterparts, confirming that spectrum sharing imposes a performance cost on both coexisting RATs. These results establish spectrum sharing as a transitional mechanism that facilitates early 5G deployment within existing LTE spectrum, rather than a long-term capacity enhancement strategy. The results are shown in Figure 4-5.

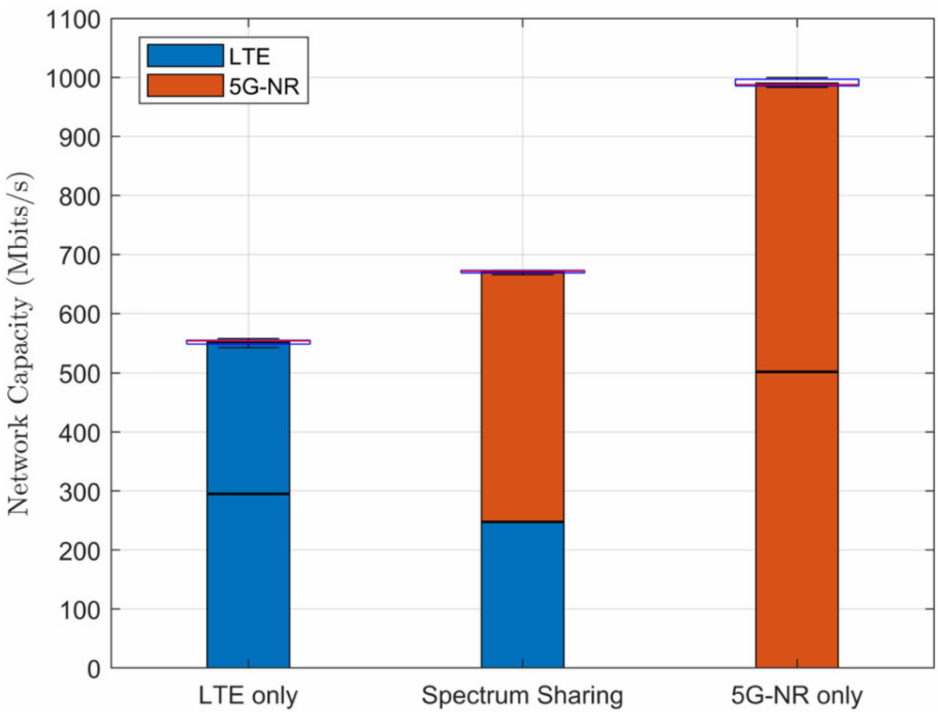

Figure 4-5 Network capacity (Mbits/s) for LTE-only, spectrum sharing, and 5G-NR-only configurations under 4×4 MIMO"

Figure 4-6 presents the impact of mixed numerology operation in LTE–5G spectrum sharing. LTE employs a fixed numerology index μ = 0, while 5G-NR operates with numerology indices μ = 0, 1, and 2, representing same-numerology and mixed-numerology coexistence configurations. These cases reflect differences in subcarrier spacing, symbol duration, and frame structure between LTE and 5G-NR, which lead to non-orthogonal resource block alignment when different numerologies are used. The figure shows that the same-numerology configuration μ(0,0) achieves higher network capacity compared to the mixed-numerology cases μ(0,1) and μ(0,2). This indicates that mixed numerology operation introduces INI, which degrades spectrum-sharing performance due to misaligned transmission structures.

Figure 4-7 extends the mixed-numerology analysis by incorporating different traffic patterns into the spectrum-sharing scenario. The figure compares full-buffer and constant-rate traffic models for the same numerology combinations considered previously. Across both traffic conditions, the same-numerology case maintains higher network capacity, while mixed-numerology configurations exhibit lower capacity. This demonstrates that INI persists under varying traffic dynamics and scheduling conditions, confirming that differences in LTE and 5G-NR frame structures introduce inherent interference limitations in spectrum-sharing environments regardless of the traffic model.

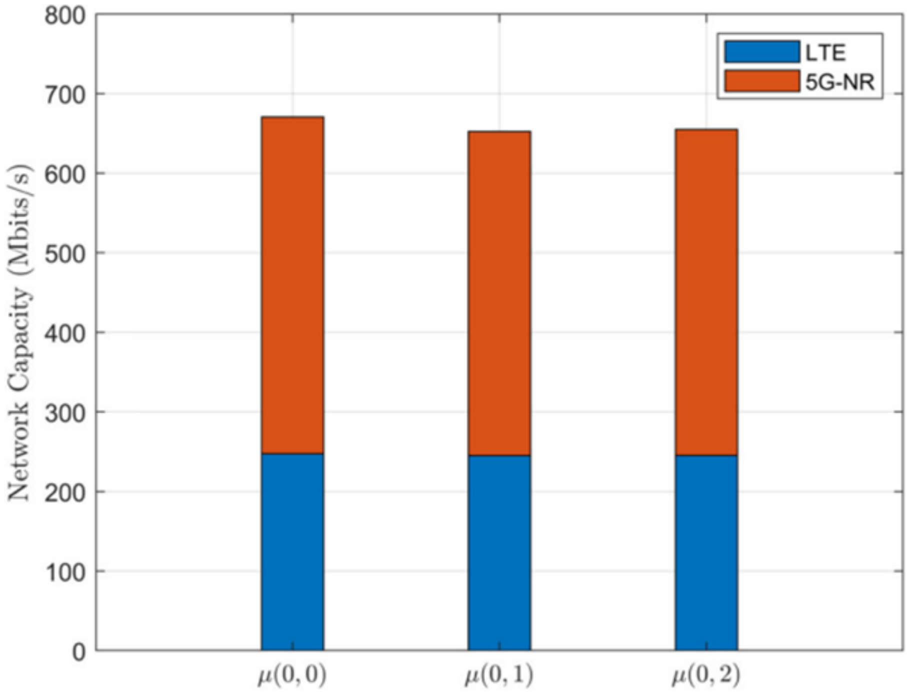

Figure 4-6 Impact of mixed numerology profiles on spectrum sharing network capacity

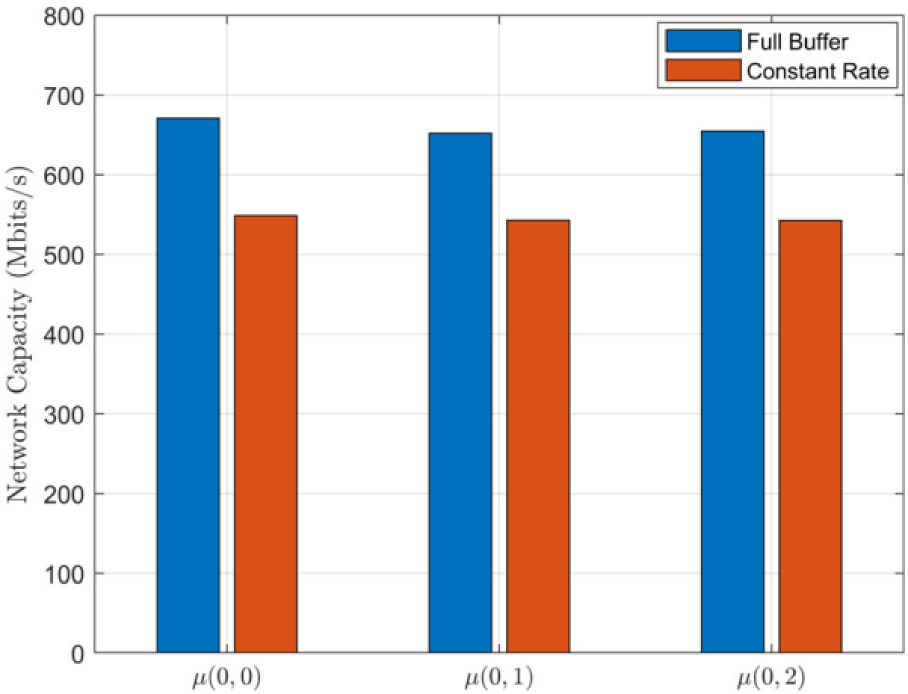

Figure 4-7 Spectrum sharing network capacity (Mbits/s) for different traffic patterns and numerologies

4.3 Scenario 3

4.3.1 Description and test setup

We consider a generic urban-like scenario for unlicensed radio use under co-channel operation in the 6 GHz band, not tied to a specific city layout, chosen to capture typical worst-case interference conditions rather than a particular deployment. Specifically, the two services 5G NR-U and Wi-Fi are investigated regarding the mutual interference caused by both services. To mitigate this interference, three different concepts are evaluated, described in the following sections.

To calculate the main quantities of interest described in Section 2.3, namely aggregate interference at the 5G NR-U BS and interference levels at the surrounding Wi-Fi devices, a simulation model is defined driven by the following assumptions: The NR-U BS is assumed to maintain seamless connectivity to multiple users, implying continuous downlink traffic and ongoing transmission activity at or near full load. For Wi-Fi devices, continuous high-volume data transmission is assumed among active devices, such that the channel is persistently occupied. Interferers are treated as contributing powers that combine incoherently, leading to a purely additive interference model. The aggregate interference at a given receiver is, consequently, given as the sum of the individual interference powers from each active interferer as specified in (4-1) where N is the total number of interferers and I_n is the individual interference power of the n-th interferer.

$$I = \sum_{n=1}^{N} I_n \tag{4-1}$$

The channel model used to calculate the received power from one device to another is a composite propagation model trat applies to each link between an NR-U BS and a Wi-Fi device, regardless of direction. The received power P_{RX} is computed as

$$P_{RX} = P_{TX} + G_{TX} + G_{RX} - 20\log\left(\frac{4\pi df}{c}\right) + PL_{ct} + PL_{tw} + PL_{in} \tag{4-2}$$

with d being the link distance, f the carrier frequency and c the speed of light. P_{TX} denotes the transmit power, G_{TX} and G_{RX} the transmit and receiver antenna gain, respectively, and PL_{ct}, PL_{tw} and PL_{in} describe additional loss terms for clutter loss, building entry loss and indoor loss, respectively, as detailed in [5].

The positions of the Wi-Fi devices and 5G NR-U BS as well as parameters relevant to signal propagation such as building entry loss, Wi-Fi transmit power and antenna height are randomly generated with a uniform distribution in a Monte Carlo simulation. The number of iterations is determined for each scenario based on the respective convergence properties encountered during simulation. Each approach is evaluated at different deployment densities ranging from 500 to 50 000 Wi-Fi devices/km^2 and in three different sub-scenarios concerning the deployment of Wi-Fi devices: By varying the ratios of indoor and outdoor Wi-Fi devices, we consider a purely outdoor scenario with no indoor devices, a hybrid scenario with an equal split as well as a purely indoor scenario with no outdoor devices. All combinations of these sub-scenarios and design parameters are part of the parameter sweep performed during the simulation. Initially, a device count matching the requested density is drawn uniformly over the 1 km² area; however, only a fraction of these devices is considered active in a given instance. Specifically, an active ratio of 0.1 is assumed, so only 10 % of the deployed Wi-Fi devices are actively transmitting at a time, intended to reflect spatial reuse behaviour as in Wi-Fi 6E/802.11ax. For a nominal density of 10 000 Wi-Fi devices/km², this leads to 1 000 simultaneously active devices after applying this 10 % ratio. The 5G NR-U BS deployment density is fixed to 1 cell/km², i.e., there is exactly one NR-U BS in the scenario area [5].

The simulations described in the following sections have been performed using a sandbox scenario written in Matlab and Python. Where possible, functionality from **TUBS**'s Simulator for Mobile Networks (SiMoNe) for modelling the scenario and calculating link properties has been adapted to this environment and utilized in the simulations that were performed.

For each combination of parameters (e.g., Wi-Fi density, indoor/outdoor deployment type), a Monte Carlo simulation with 10 000 independent iterations is performed. Each iteration follows a fixed sequence:

1. Draw positions of the single NR-U BS and all Wi-Fi devices uniformly within the 1 km² area.
2. For deployment configurations that include both indoor and outdoor Wi-Fi, independently assign each Wi-Fi device as indoor or outdoor according to the specified ratio.
3. For each indoor Wi-Fi device, randomly draw a building entry loss value uniformly between $PL_{ct,min}$ and $PL_{ct,max}$, and an indoor depth d_{in} uniformly between 0 m and 25 m, then compute the corresponding indoor loss PL_{in}.
4. Randomly assign each active Wi-Fi device a transmit power within a prescribed range from 0 dBm up to the maximum 23 dBm.
5. For each interference link between the NR-U BS and each active Wi-Fi device (in both directions), generate an individual clutter loss PL_{ct} from the ITU-R P.2108-1-based model, considering geometry and an obstructed-location random factor.
6. Use the complete link budget formula to compute the received interference power for each link, including antenna gains and radiation patterns.
7. For NR-U BS interference evaluation, sum all contributions from Wi-Fi interferers to get the aggregate interference for that iteration; for Wi-Fi interference evaluation, record the interference power at each Wi-Fi device from the NR-U BS.

4.3.1.1 Exclusion Zone

The key design element of this mitigation concept is a circular geolocation-based exclusion zone in which Wi-Fi devices are not allowed to operate. The radius of this exclusion zone is the main design parameter, varied from 0 m to 700 m in steps of 50 m. Figure 4-8 shows an exemplary realization of one iteration in the Monte Carlo simulation for a deployment density of 5 000 Wi-Fi devices/km² and an active ratio of 0.1.

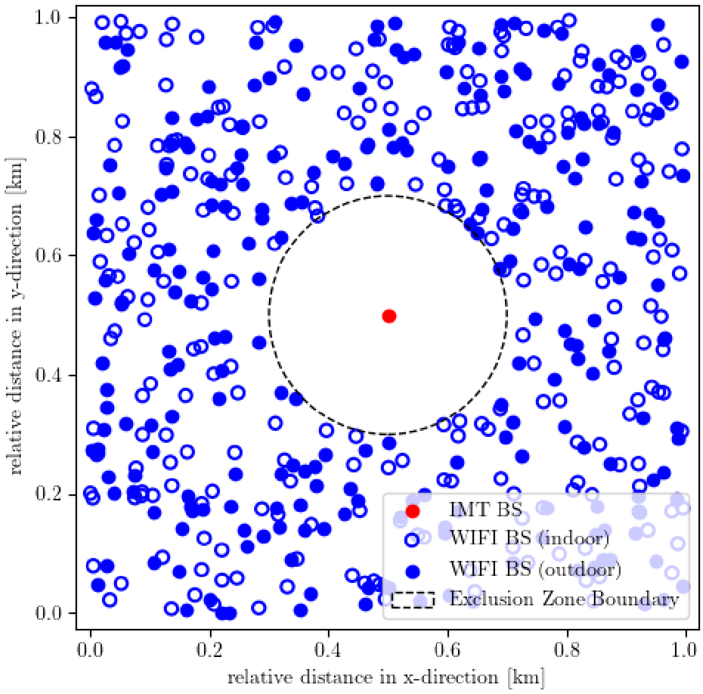

Figure 4-8 Example constellation of a 5G NR-U BS and both indoor and outdoor Wi-Fi devices with a density of 5000 devices/km² and an active ratio of 0.1 constrained by a geographical exclusion zone with a radius of 200 m.

Wi-Fi devices are deployed in a hybrid scenario, indoor devices being represented by hollow circles and outdoor devices by full circles. The exclusion zone has a radius of 200 m and prevents any Wi-Fi devices from being active inside its boundary. The remaining simulation parameters, including all values of the parameter sweep, are denoted in Table 4-3 [5]. Every combination of parameters has been considered in a Monte Carlo simulation with 10 000 iterations.

Table 4-3 Simulation parameters

Category	Parameter	Value
Common	Carrier frequency	6.775 GHz
	Scenario dimensions	1 km^2
	Building entry loss	[13.57, 31.23] dB [8]
	Exclusion zone radius	{0, 50, …, 700} m
	Clutter loss	ITU-R P.2108-1 [9]
5G NR-U	Transmit power	24dBm [10]
	Antenna gain	5dBi [10]
	Radiation pattern	Omni directional [11]
	Maximum interference	-179.6 dBm/Hz [12]
	Antenna height	20 m [10]
	Deployment density	1 cells/km^2
Wi-Fi	Max transmit power	23 dBm [13]
	Antenna gain	0 dBi
	Radiation pattern	Omni directional
	Indoor density ratio	0 / 0.5 / 1
	Outdoor density ratio	1 / 0.5 / 0
	Active ratio	0.1
	Antenna height	[0, 15] m
	Deployment density	500 / 1000 / 5000 / 10000 / 50000 devices/km^2

4.3.1.2 MVDR Beamforming

The simulation environment for the MVDR beamforming approach is very similar to the one used in the previous exclusion zone approach. This is by design, to facilitate comparisons between the different approaches. Figure 4-9 shows an exemplary realization of one iteration in the Monte Carlo simulation for a deployment density of 5 000 Wi-Fi devices/km^2 and an active ratio of 0.1. Wi-Fi devices are deployed in a hybrid scenario, indoor devices being represented by hollow circles and outdoor devices by full circles. There is no exclusion zone present, so any Wi-Fi device may be generated arbitrarily close to the 5G NR-U BS within the simulation area of 1 km^2.

The key idea of this approach is to adopt an MVDR beamformer as described in [6] at the 5G NR-U BS to mitigate interference from Wi-Fi devices. This is attempted by introducing nulls in the beamforming diagram at directions with the most interference caused by surrounding Wi-Fi devices as described below.

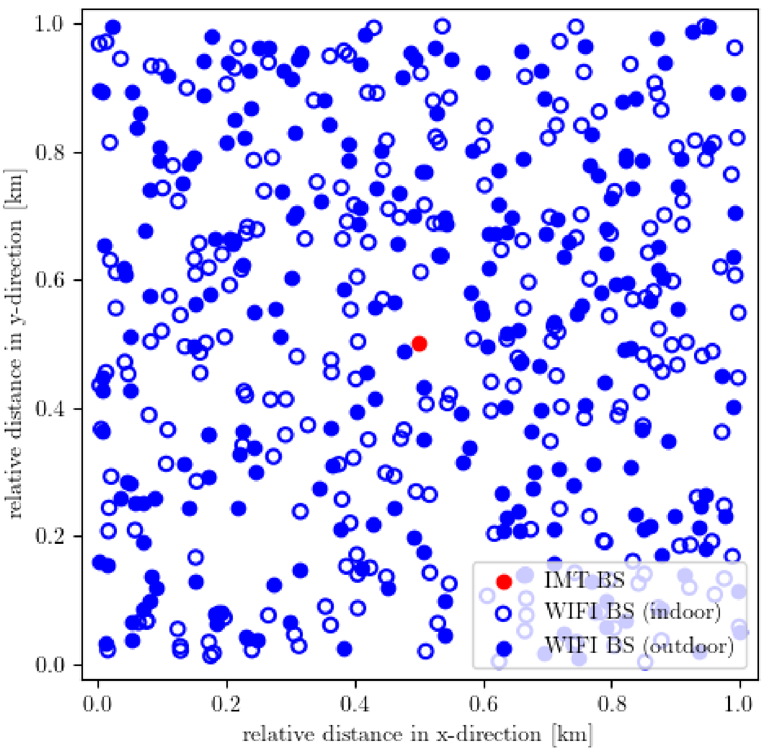

Figure 4-9 Example constellation of a 5G NR-U BS and both indoor and outdoor Wi-Fi devices with a density of 5000 devices/km2 and an active ratio of 0.1.

At the core of an MVDR beamformer is an ULA with M identical antennas placed on a straight line with equal distances d. Beamforming in general introduces multiplicative complex beamforming weights to the signals transmitted at each antenna in the ULA. Regular beamforming determines these weights as simple equal phase offsets between each pair of antennas in the array which are represented as the steering vector $\boldsymbol{a}(\theta_0)$ in (4-3) where θ_0 is the direction of the main lobe of the beam.

$$\boldsymbol{a}(\theta_0) = (1 \quad e^{-j\pi\sin(\theta_0)} \quad e^{-j2\pi\sin(\theta_0)} \quad \dots \quad e^{-j(M-1)\pi\sin(\theta_0)})^T \tag{4-3}$$

In contrast, the MVDR beamforming algorithm uses a different process to determine the beamforming weights which enables introducing high attenuation for specific directions, called nulls, in addition to steering the main beam lobe. The MVDR beamforming weights result from the optimization problem in (4-4) where $\boldsymbol{w}$ denotes the vector of beamforming weights and $\widehat{\boldsymbol{R}}_{xx}$ is the sample covariance matrix of the input signal to the beamformer. The problem aims to minimize the total signal energy under the constraint that the antenna factor in the direction of the main lobe is 1.

$$\min_{\boldsymbol{w}} \boldsymbol{w}^H \widehat{\boldsymbol{R}}_{xx}\boldsymbol{w}, \quad s.t.\ \boldsymbol{w}^H\boldsymbol{a}(\theta_0) = 1 \tag{4-4}$$

The solution to this optimization problem can be obtained by applying the Lagrange method and is given in (4-5) for a known value of $\boldsymbol{R}_{xx}$. Since the covariance matrix $\boldsymbol{R}_{xx}$ does not exist for the transmitting side, it can be substituted as shown in (4-6), where $\boldsymbol{a}(\theta_i)$ are the steering vectors for all I null angles to be introduced and σ_n^2 represents the noise power at the transmitter [6].

$$\boldsymbol{w}_{MVDR} = \frac{\boldsymbol{R}_{xx}^{-1}\boldsymbol{a}(\theta_0)}{\boldsymbol{a}^H(\theta_0)\boldsymbol{R}_{xx}^{-1}\boldsymbol{a}(\theta_0)} \tag{4-5}$$

$$\boldsymbol{R}_{xx} = \boldsymbol{a}(\theta_0)\boldsymbol{a}^H(\theta_0) + \sum_{i=1}^{I}\boldsymbol{a}(\theta_i)\boldsymbol{a}^H(\theta_i) + \sigma_n^2\boldsymbol{I} \tag{4-6}$$

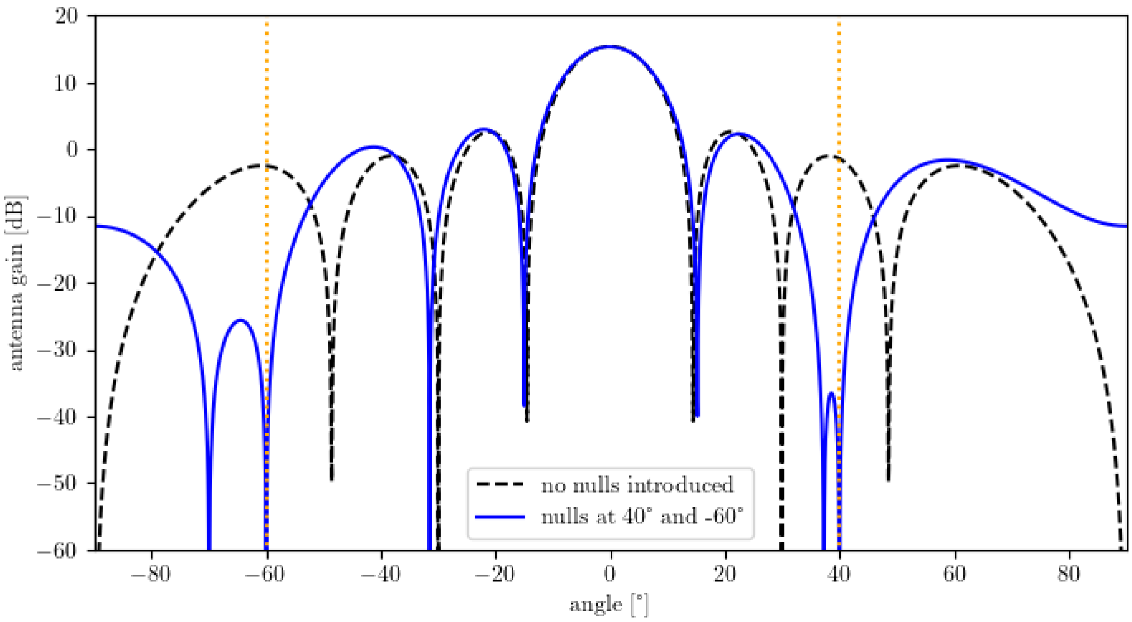

Figure 4-10 Antenna gain of an MVDR beamforming antenna directed to 0° and two nulls at 40° and -60° in comparison to an antenna directed in the same direction with no nulls introduced

Assuming far-field conditions, the resulting beamforming weights determine the azimuthal antenna factor via $AF(\theta) = \boldsymbol{w}_{MVDR}^{H}\boldsymbol{a}(\theta)$. An example MVDR beamforming diagram for a beam with a main lobe direction of 0° and two nulls at 40° and -60° is shown in Figure 4-10, compared to a regular beamforming diagram with the same main lobe direction, but without introducing any nulls.

In the simulation, the number of introduced nulls is considered as a design parameter and part of the parameter sweep detailed in Table 4-4. For a given number of nulls to be introduced, the respective angles are calculated by examining the received interference power from the surrounding Wi-Fi devices: The power levels of all devices are first windowed with respect to their angle of arrival in an interval of $\pm 1°$ around any given angle. The nulls are then introduced iteratively by placing a null at the angle where the windowed interference power is maximal. The range of $\pm 5°$ surrounding that angle is excluded from the future search space in order to avoid multiple nulls in close proximity. These two steps are repeated until the desired number of nulls has been introduced, after which the beamforming weights can be computed. The direction can be chosen independently of the surrounding Wi-Fi devices since it is used to direct the beam at specific 5G NR-U UE. However, since 5G NR-U UE are not considered in this specific scenario, the main lobe direction is arbitrarily chosen to be the direction of least interference by the surrounding Wi-Fi devices. As the beamforming diagram can only meaningfully be evaluated in an interval of 180°, the simulation assumes two sectors at the 5G NR-U BS, encompassing 180° each, split into a northern and a southern sector. The MVDR beamforming process is performed separately for each of the sectors in order to cover the full 360° field of view at the 5G NR-U BS. Every combination of parameters has been considered in a Monte Carlo simulation with 100 000 iterations.

Table 4-4 Simulation parameters for MVDR beamforming

Category	Parameter	Value
Common	Carrier frequency	6.775 GHz
	Scenario dimensions	1 km^2
	Building entry loss	[13.57, 31.23] dB [8]
	Clutter loss	ITU-R P.2108-1 [9]

5G NR-U	Transmit power	24dBm [10]
	Antenna gain	5dBi [10]
	Radiation pattern	MVDR beam
	Number of antennas	8 [6]
	Number of nulls introduced	{1, 2, …, 10, 15, 20, 25, 30, 40, 50}
	Maximum interference	-179.6 dBm/Hz [12]
	Antenna height	20 m [10]
	Deployment density	1 cells/km²
Wi-Fi	Max transmit power	23 dBm [13]
	Antenna gain	0 dBi
	Radiation pattern	Omni directional
	Indoor density ratio	0 / 0.5 / 1
	Outdoor density ratio	1 / 0.5 / 0
	Active ratio	0.1
	Antenna height	[0, 15] m
	Deployment density	500 / 1000 / 5000 / 10000 devices/km²

4.3.1.3 Tracking Individual UE using Narrow Beams

The UE tracking approach extends the previous simulation environments by introducing 5G NR-U UE (in both indoor and outdoor environments) in addition to the Wi-Fi devices that have already been introduced previously. Figure 4-11 shows an exemplary realization of a single simulation iteration for a deployment density of 5 000 Wi-Fi devices/km² and an equal number of 5G NR-U UE in combination with an active ratio of 0.1. Similar to Wi-Fi devices, 5G NR-U UE are displayed as full orange circles for outdoor devices and hollow circles for indoor devices.

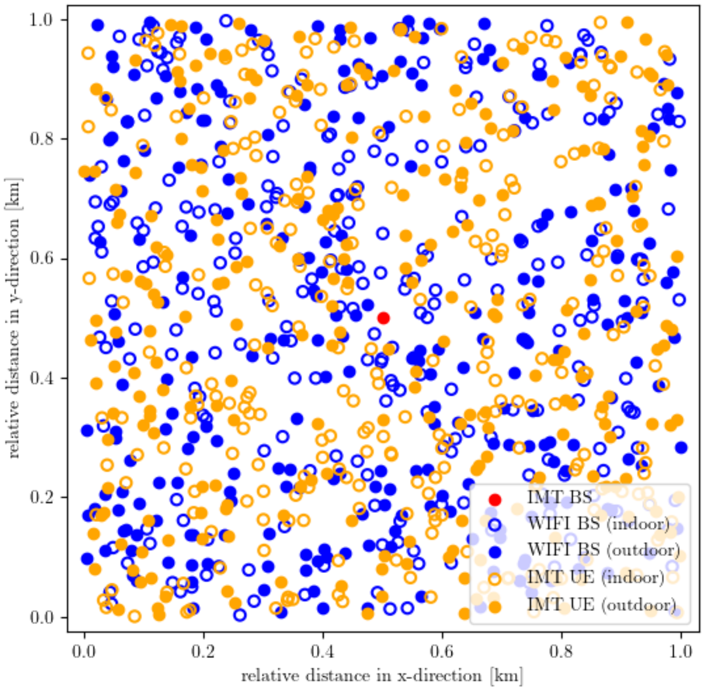

Figure 4-11 Example constellation of a 5G NR-U BS and both indoor and outdoor Wi-Fi devices with a density of 5000 devices/km² and an active ratio of 0.1 as well as 5G NR-U UE with the same density

The 5G NR-U UE included in this simulation design are used by the 5G NR-U BS to narrowly focus the transmit power to individual UE in an effort to evaluate the impact of this technique on the interference caused by the 5G NR-U BS at the surrounding Wi-Fi devices. To accomplish this, the simulation uses Gaussian beams for each 5G NR-U UE as introduced in section 3.2. As specified in [7], assuming far-field conditions, the electric field distribution can be computed for any given angle relative to the direction of propagation using equation (4.7), where $E(\theta)$ denotes the magnitude of the electric field at an angular offset of θ degrees off the propagation direction and θ_0 denotes the far-field divergence angle which can be represented by the half-power beam width via the identity $\theta_{HPBW} = 1.18 \cdot \theta_0$.

$$\frac{E(\theta)}{E(0)} = \exp\left(-\left(\frac{\theta}{\theta_0}\right)^2\right) \tag{4-7}$$

Such a beam is generated for every 5G NR-U UE in the simulation scenario, which are subsequently combined into one beamforming diagram additively after being weighted to compensate for the differences in the expected link budgets. An example of a resulting beamforming diagram is shown in Figure 4-12 b) for a low-density deployment scenario shown in Figure 4-12 a).

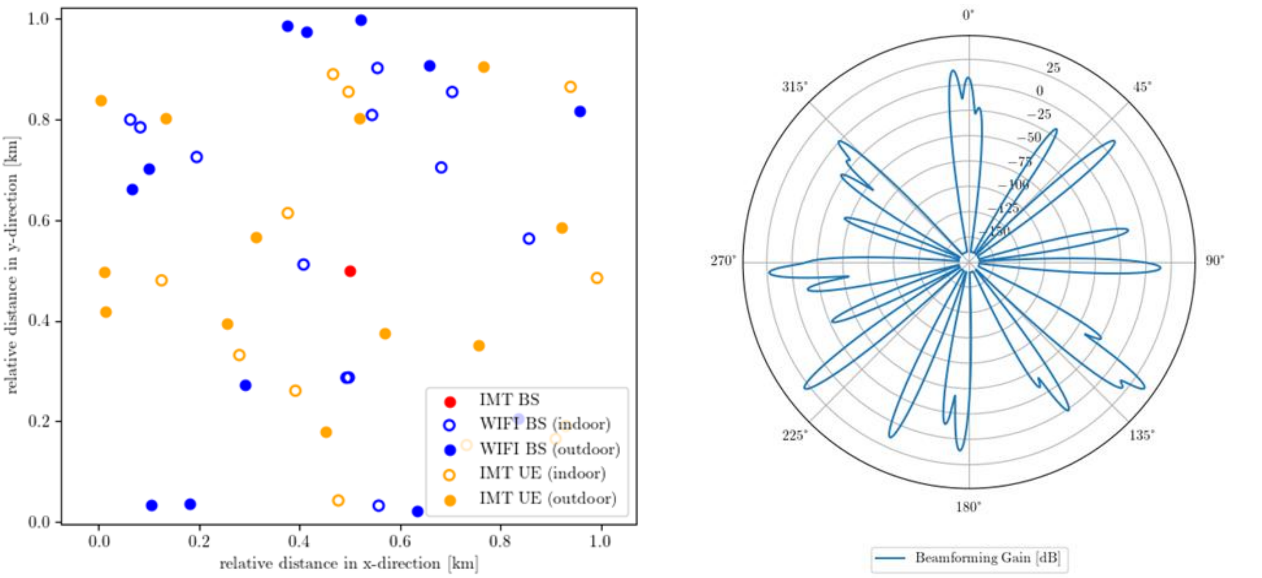

a) b)

Figure 4-12 Gaussian beam tracking approach, a) Example low-density constellation of a 5G NR-U BS, 5G NR-U UE and Wi-Fi devices, b) resulting beamforming diagram using 2° wide gaussian beams to track individual 5G NR-U UE

Beyond the parameters already described in previous sections, the UE tracking approach considers the half-power beam width as a design parameter and evaluates a range of values from 1° to 30°. Table 4-5 shows the full set of parameters used in the simulation and the parameter sweep. Every combination of parameters has been considered in a Monte Carlo simulation with 100 000 iterations.

Table 4-5 Simulation parameters for Gaussian beamforming

Category	Parameter	Value
Common	Carrier frequency	6.775 GHz
	Scenario dimensions	1 km^2
	Building entry loss	[13.57, 31.23] dB [8]
	Clutter loss	ITU-R P.2108-1 [9]
5G NR-U	Transmit power	24dBm [10]

	Antenna gain	5dBi [10]
	Radiation pattern	gaussian beams
	Beam width (HPBW)	{1, 2, 4, 6, 8.5, 9.5, 11.5, 20, 30}
	Maximum interference	-179.6 dBm/Hz [12]
	Antenna height	20 m [10]
	Deployment density	1 cells/km^2
Wi-Fi	Max transmit power	23 dBm [13]
	Antenna gain	0 dBi
	Radiation pattern	Omni directional
	Indoor density ratio	0 / 0.5 / 1
	Outdoor density ratio	1 / 0.5 / 0
	Active ratio	0.1
	Antenna height	[0, 15] m
	Deployment density	500 / 1000 / 5000 / 10000 devices/km^2

4.3.2 Simulation and Test Results

This subsection analyses the effectiveness of three different interference mitigation approaches for co-channel operation between 5G NR-U and Wi-Fi systems in the 6 GHz band. Exclusion zone simulations demonstrate that outdoor Wi-Fi deployments require prohibitively large radii (600-700 m) to achieve acceptable interference levels, while indoor deployments benefit significantly from building penetration losses and can coexist with more modest exclusion zones (150-300 m). Advanced beamforming techniques – MVDR with adaptive nulling and narrow Gaussian beam tracking – show promising interference reduction in low-to-medium density scenarios (up to 7-13 dB improvement), but their performance gains diminish substantially at high deployment densities above 5,000 devices/km², indicating that hybrid approaches combining multiple mitigation strategies will be necessary for dense urban environments.

4.3.2.1 Exclusion Zone

The simulation using an exclusion zone to mitigate interference is evaluated from two distinct points of view: Firstly, the impact on the interference at the IMT 5G NR-U BS, quantified by the resulting aggregate interference from the surrounding Wi-Fi devices, shown in Figure 4-13. Secondly, the impact on the interference on the surrounding Wi-Fi devices caused by the 5G NR-U BS, depicted in Figure 4-14.

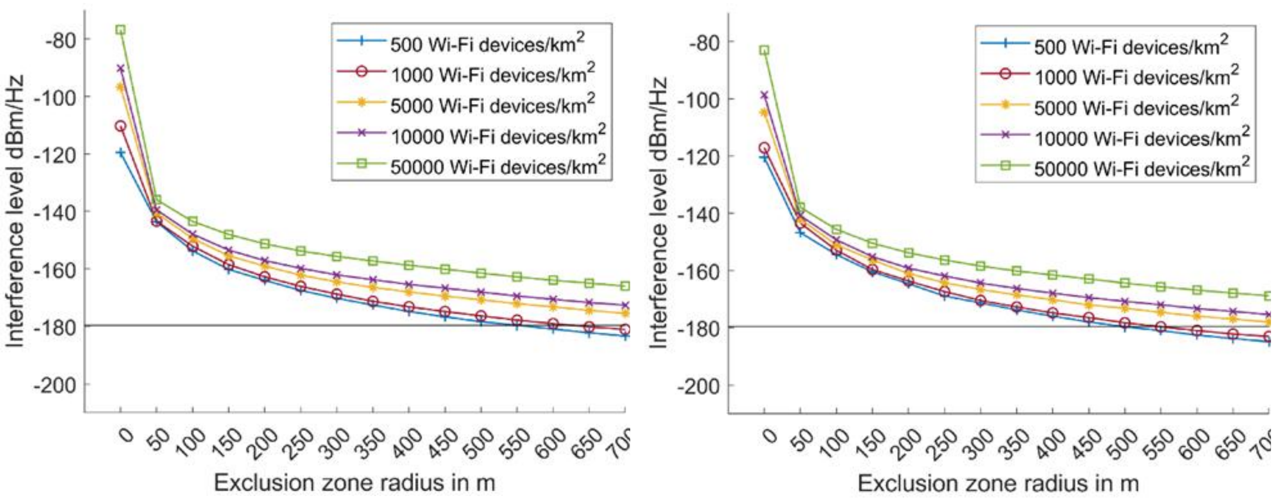

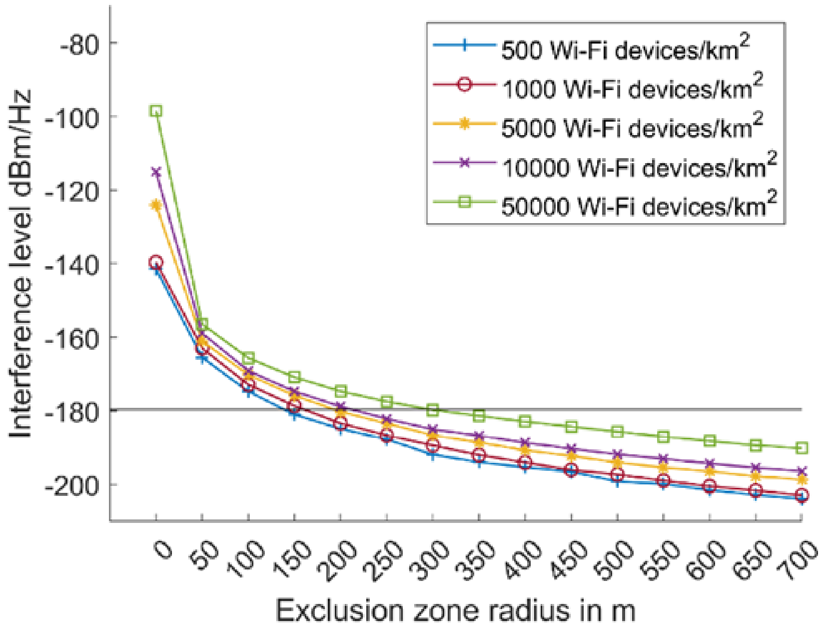

Figure 4-13 Simulation results using an exclusion zone approach with Wi-Fi devices being deployed a) outdoors only, b) indoors and outdoors (uniformly distributed), c) indoors only, as illustrated in [5].

For outdoor Wi-Fi deployments (Figure 4-13 a), even when applying a circular exclusion zone of several hundred m of radius, the resulting aggregate interference at the NR-U BS often exceeds the maximum interference threshold of −179.6 dBm/Hz obtained from ITU-R sharing studies [14], so co-channel operation becomes infeasible without additional coordination mechanisms. In hybrid indoor-outdoor Wi-Fi deployments (Figure 4-13 b), the presence of indoor devices reduces the average interference level due to building entry and indoor propagation losses, but the high-interference tail remains significant enough that exclusion zones alone do not reliably guarantee protection of the NR-U BS under dense deployments. Only in the pure indoor Wi-Fi deployment scenario (Figure 4-13 c) does the combination of building penetration loss, indoor attenuation, and a moderate exclusion zone (roughly 150–300 m depending on Wi-Fi density) reduce the upper-percentile aggregate interference below the allowed threshold, thus enabling robust co-channel coexistence without more advanced spectrum sharing [5].

The tolerance range for interference levels at Wi-Fi devices is approximated in [5] between about −91 dBm (20 MHz) and −75 dBm (320 MHz) based on 802.11ax performance figures [15]. For outdoor Wi-Fi deployments in dense scenarios (e.g., 50 000 devices/km²), and in the absence of an exclusion zone, a non-negligible fraction of Wi-Fi links – on the order of tens of percent for narrower channels – can experience interference above this threshold, particularly at smaller link budgets, which may degrade throughput or connectivity. As visualized in Figure 4-14, introducing a large exclusion zone (on the order of 600–700 m) around the NR-U BS substantially reduces the probability that Wi-Fi devices observe interference above their tolerance range, effectively enabling co-channel operation of Wi-Fi and NR-U in the considered outdoor scenarios. For indoor Wi-Fi deployments, additional building entry and indoor losses again provide significant isolation; with an exclusion zone of approximately 300 m around the NR-U BS, interference at Wi-Fi receivers generally remains below the derived thresholds across the simulated distribution, making coexistence substantially less critical than at the NR-U BS side [5].

4.3.2.2 MVDR Beamforming

This section presents the results using an MDVR beamforming approach in the simulation. Figure 4-15 shows the average aggregate interference at the 5G NR-U BS over all 10 000 iterations in an outdoor-only deployment. We can make several key observations from this figure: considering different numbers of interference directions while calculating the MVDR beamforming diagram, it is apparent for all densities that the resulting interference levels lower with an increasing number of considered interference directions, but only up to a certain point between 5 and 10 directions. Past this minimum, the interference levels rise again, until they approach a constant value starting at around 25 directions.

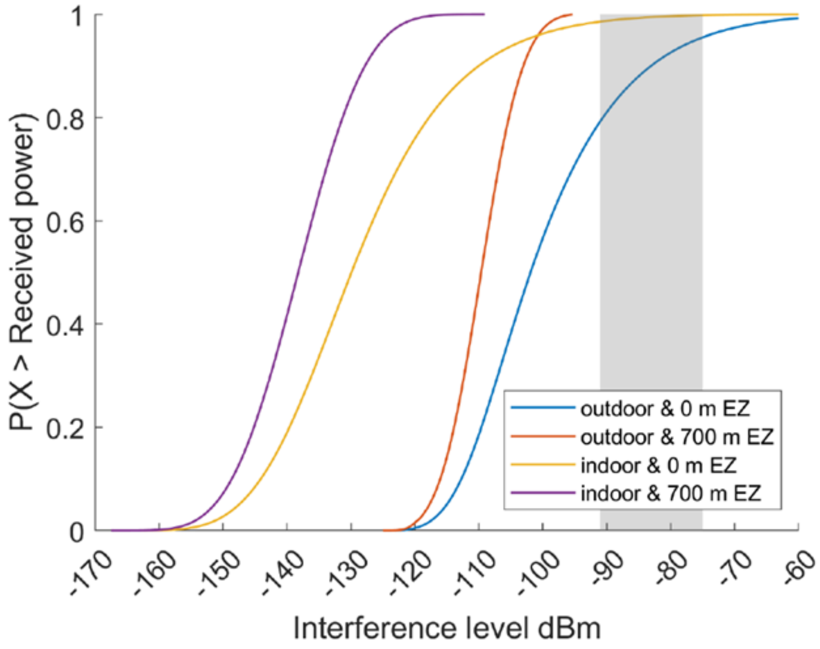

Figure 4-14 Cumulative Distribution Function (CDF) of interference levels at Wi-Fi devices caused by a 5G NR-U BS for outdoor and indoor deployments with and without an exclusion zone.

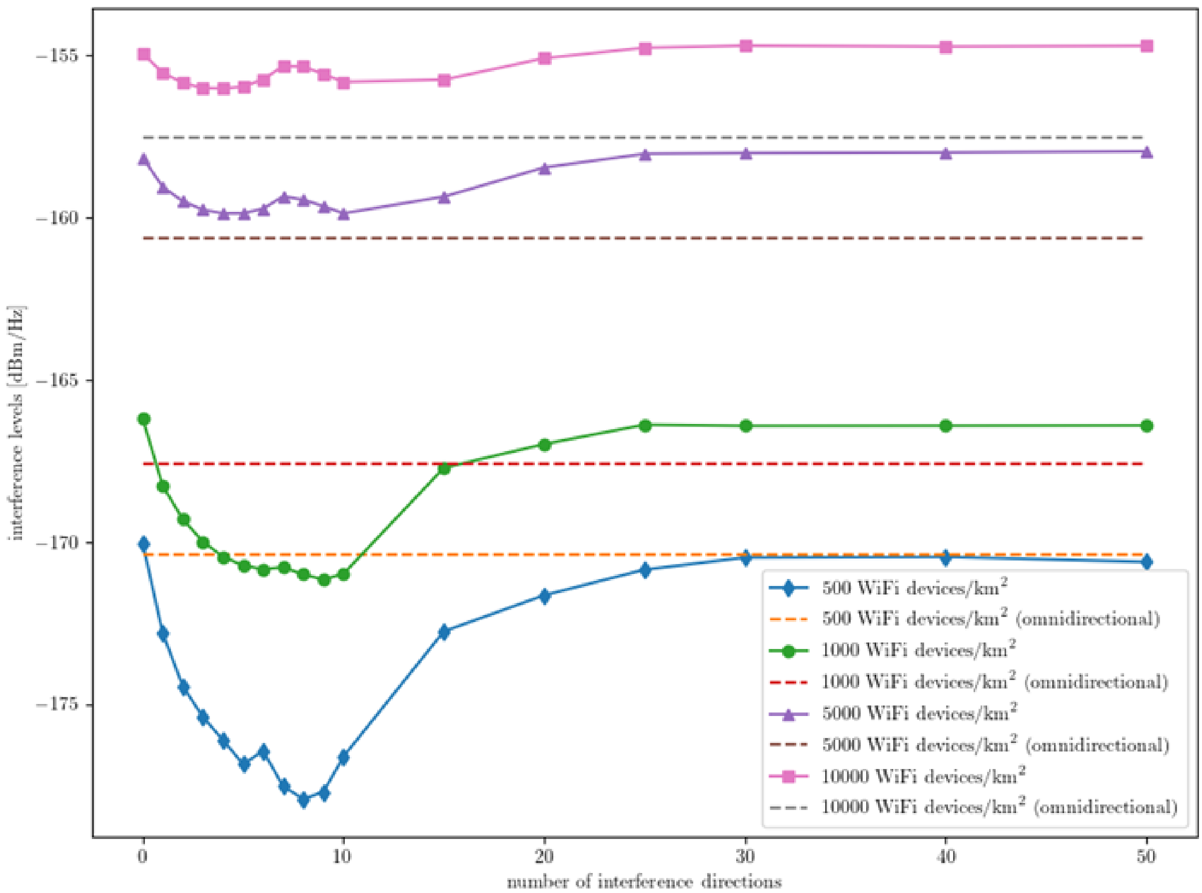

Figure 4-15 Aggregate interference levels at the 5G NR-U BS caused by the surrounding Wi-Fi devices with different deployment densities (outdoor only) utilizing MVDR beamforming at the 5G NR-U BS compared to an omnidirectional antenna.

Comparing the different deployment densities of Wi-Fi devices, we observe that the aggregate interference levels rise with increasing deployment density. Simultaneously, the difference between the interference level of an omnidirectional antenna and the minimum interference level using MVDR beamforming decreases from 7.53 dB/Hz at a Wi-Fi deployment density of 500 devices/km^2 to 3.57 dB/Hz at a density of 1 000 devices/km^2, until the interference level using MVDR surpasses the omnidirectional case beginning at a density of 5 000 devices/km^2.

Figure 4-16 depicts the aggregate interference levels at the 5G NR-U BS in a hybrid indoor and outdoor deployment of Wi-Fi devices, while both deployment types each account for 50% of the simulated devices. The figure shows similar qualitative results compared to the outdoors-only scenario. However, the aggregate interference levels for all considered deployment densities are lower than in the outdoor-only scenario. This is most likely due to additional building penetration losses and indoor propagation losses introduced by indoor Wi-Fi devices. In consequence, the hybrid scenario is the first one, where MVDR beamforming reduces the interference level below the tolerance threshold of −179.6 dBm/Hz discussed in the previous section for a deployment density of 500 devices/km^2. Additionally, the hybrid deployment scenario improves the difference between the minimum aggregated interference level and the omnidirectional case to 11.83 dB/Hz for a deployment density of 500 devices/km^2, 6.99 dB/Hz at 1 000 devices/km^2 and 0.63 dB/Hz at 5 000 devices/km^2. The MVDR approach only stops outperforming the omnidirectional case starting at a deployment density of 10 000 devices/km^2.

Finally, Figure 4-17 contains the results for the indoor-only deployment of Wi-Fi devices. Once again, the overall trends in the individual graphs remain the same, compared to the previous two scenarios. Since this scenario considers only indoor Wi-Fi devices, the effects of the increased losses during propagation inside buildings and building penetration are even more pronounced, resulting in even lower aggregate interference values overall. This leads to another increase in the difference between the minimum aggregated interference level and the omnidirectional case from 13.19 dB/Hz at a deployment density of 500 devices/km^2 to 0.77 dB/Hz at 10 000 devices/km^2. This makes this scenario the only one, where MVDR beamforming outperforms an omnidirectional antenna even in high-density deployment scenarios.

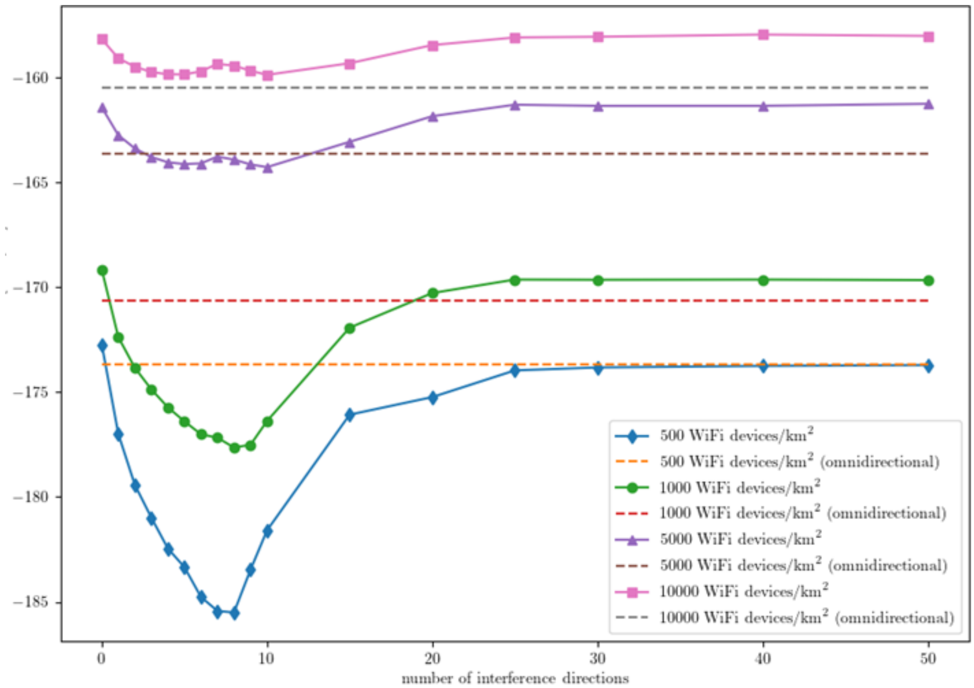

Figure 4-16 Aggregate interference levels at the 5G NR-U BS caused by the surrounding Wi-Fi devices with different deployment densities (hybrid indoor and outdoor) utilizing MVDR beamforming at the 5G NR-U BS compared to an omnidirectional antenna.

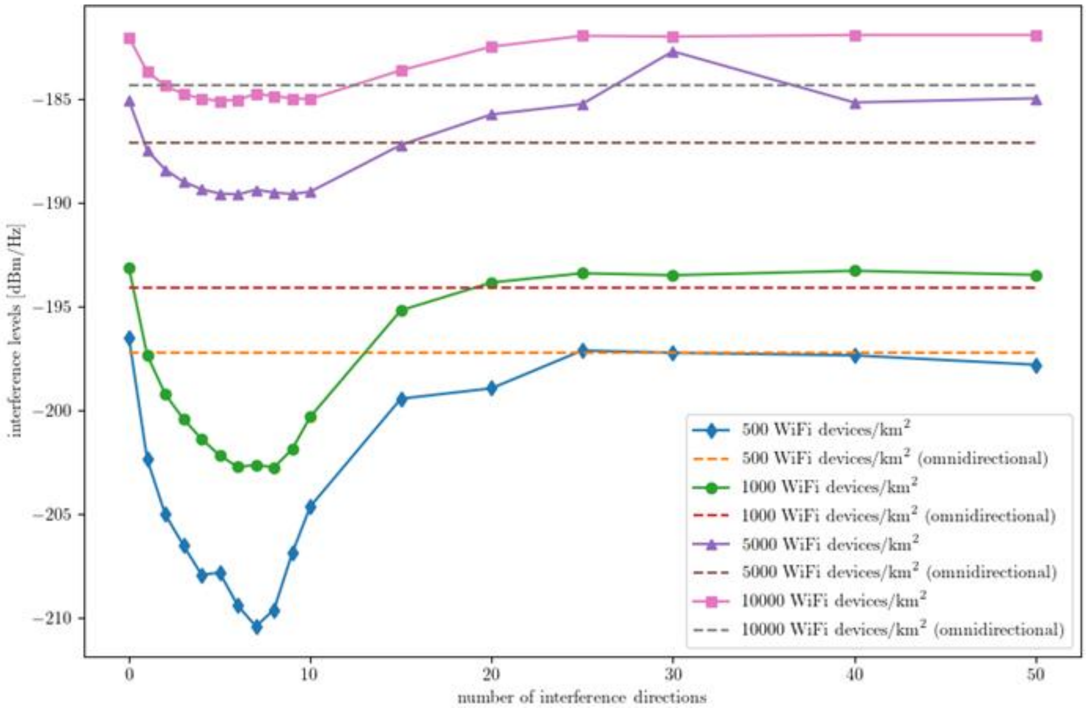

Figure 4-17 Aggregate interference levels at the 5G NR-U BS caused by the surrounding Wi-Fi devices with different deployment densities (indoor only) utilizing MVDR beamforming at the 5G NR-U BS compared to an omnidirectional antenna

Overall, the results indicate that MVDR beamforming can reduce aggregate interference at a 5G NR-U BS caused by surrounding Wi-Fi devices under co-channel operation in the 6 GHz band. However, the performance gain diminishes quickly in dense deployment scenarios, which is especially relevant for scenarios with a low number of indoor devices compared to outdoor devices. In a part of these scenarios, where the minimum aggregate interference level is below the omnidirectional interference level, but still above the tolerance threshold of −179.6 dBm/Hz, MVDR beamforming can still be used in combination with other interference mitigation approaches to improve the resulting interference compared to an omnidirectional antenna. This may even affect some scenarios with a lower deployment density under realistic conditions, as multipath propagation may cause a more diffuse set of incoming signals at the 5G NR-U BS which may increase the difficulty of attenuating specific Wi-Fi devices using MVDR nulls.

4.3.2.3 Tracking Individual UE using Narrow Beams

In this section, the effects of using narrow Gaussian beams to track 5G NR-U UE on the interference at the Wi-Fi devices surrounding the 5G NR-U BS is evaluated. Similar to the previous simulation on MVDR beamforming, this simulation surveys a number of design parameters whose impact on the resulting interference levels is part of the evaluation.

The First design parameter under consideration is the width of the beams that are used by the 5G NR-U BS to track individual 5G NR-U UE. This quantity is given as the half-power beam width (HPBW), defined as double the angle between the direction of the highest signal strength and the direction at which the beam signal strength first reaches half the power of the highest signal strength. Figure 4-18 shows the resulting interference levels at all Wi-Fi devices caused by a 5G NR-U BS using Gaussian beams with varying HPBW from 1° to 30°, displayed as the cumulative distribution function. The figure is split into three parts, each corresponding to the ratio of the number of indoor Wi-Fi devices to the number of outdoor devices: Figure 4-18 a) describes a scenario with outdoor devices only, Figure 4-18 b) shows a hybrid scenario where half of the devices are deployed outdoors and the other half indoors, finally, Figure 4-18 c) shows the indoor-only deployment scenario.

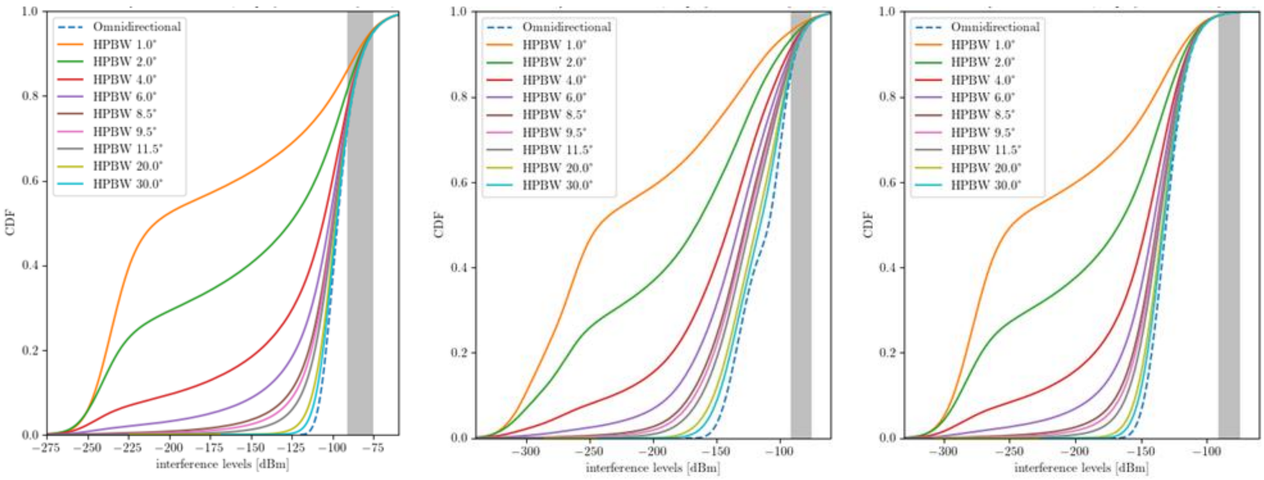

Figure 4-18 Cumulative distribution function of the interference levels at the Wi-Fi devices deployed with a density of 500 Wi-Fi devices/km^2 using gaussian beams with different beam widths at the 5G NR-U BS compared to the distribution of an omnidirectional antenna in, a) an outdoor-only scenario, b) a hybrid indoor and outdoor scenario, c) an indoor-only scenario

From Figure 4-18, it is apparent that the UE tracking approach using narrow Gaussian beams outperforms an omnidirectional antenna for all considered beam widths. The resulting interference levels at the Wi-Fi devices improve with narrower beam widths, while the interference levels for broader beams near 30° approach the levels observed in the omnidirectional case. While the interference levels using UE tracking improve in all cases compared to an omnidirectional antenna, the interference thresholds of -91 dBm for bandwidths of 20 MHz and -75 dBm for bandwidths of 320 MHz outlined in [5] and marked as a gray area in Figure 4-18 are only reliably reached in an indoor-only deployment scenario with fewer than 1% of Wi-Fi devices experiencing interference levels that surpass these thresholds. In both the hybrid and the outdoor-only scenario, UE tracking improves the interference levels compared to an omnidirectional antenna, but only to a certain degree: while the narrowest beams only keep 95% of Wi-Fi devices below the lowest interference threshold compared to 85% with an omnidirectional antenna in hybrid deployments, only 85% of Wi-Fi devices are below the threshold in the outdoor-only scenario compared to 70% of devices when using an omnidirectional antenna. This feeds into the general observation that interference levels rise with the number of deployed outdoor Wi-Fi devices due to non-existent building penetration losses as well as indoor propagation losses. At the interference threshold for bandwidths of 320 MHz, the difference between beam widths and the omnidirectional case reduces considerably.

The next design parameter to be evaluated is the deployment density of Wi-Fi devices as well as 5G NR-U UE. Both densities have been modeled dependently: The density of Wi-Fi devices is specified as an absolute value, while the density of 5G NR-U UE is specified as a factor of the Wi-Fi device density.

Figure 4-19 shows the cumulated distribution functions of the interference levels at Wi-Fi devices under varying deployment densities, compared to the interference levels of an omnidirectional antenna. For clarity, only the lowest interference levels (best case) over all densities are shown in the graph for the omnidirectional antenna along with only two values of HPBW (1° and 11.5°). This allows for the following observations: while around 95% of Wi-Fi devices clear the interference threshold for 320 MHz channels in all considered cases, the impact of UE tracking becomes apparent when considering the threshold for 20 MHz channels. Here, we notice a gradient in the interference levels for different deployment densities and beams with a HPBW of 1° from 86% of devices below the interference threshold at a density of 500 Wi-Fi devices/km^2 to 81.5% of devices below the threshold at 1 000 Wi-Fi devices/km^2. We also observe that, starting from a deployment density of 5 000 Wi-Fi devices/km^2, the difference to the omnidirectional case becomes marginal at 74% of devices under the interference level threshold.

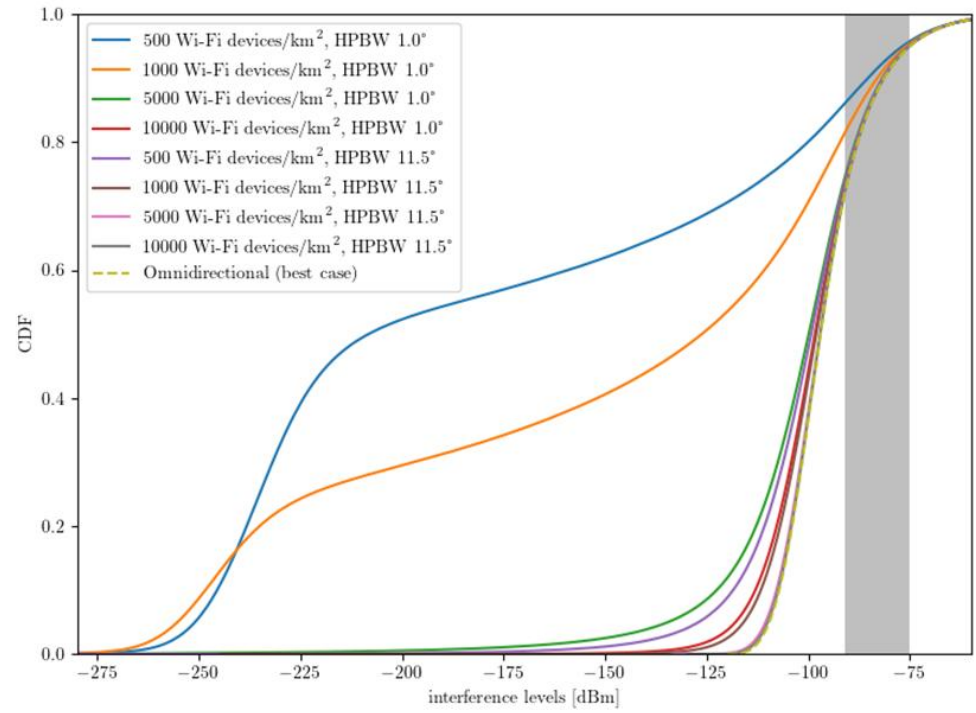

Figure 4-19 Cumulative distribution function of the interference levels at the Wi-Fi devices deployed with different densities using gaussian beams with a beam width of 1° and 11.5° compared to the distribution of an omnidirectional antenna in an outdoor-only scenario.

While the distributions described in Figure 4-19 are simulated for a constant ratio of 1 between the number of Wi-Fi devices and the number of 5G NR-U UE, this ratio is varied in Figure 4-20 for a constant density of 500 Wi-Fi devices/km^2. For clarity, only the lowest interference levels (best case) over all densities are shown in the graph for the omnidirectional antenna. Figure 4-20 shows a clear improvement of all considered ratios over the omnidirectional case. At the interference threshold for 20 MHz bandwidths, a ratio of 0.1 5G NR-U UE per Wi-Fi device enables 97% of Wi-Fi devices to remain below the threshold. This value decreases with rising ratios to 94% at a ratio of 0.25, 90.5% at 0.5, 86% at a ratio of 1 down to 81.5% for a ratio of 2. The UE to Wi-Fi ratio is the first parameter that yields a noticeable difference even at the threshold for 320 MHz channels, where 98% of Wi-Fi devices clear the threshold for a ratio of 0.1 and only 95.5% of Wi-Fi devices for a ratio of 2.

In summary, the results show that tracking individual 5G NR-U UE using narrow Gaussian beams can reduce interference levels caused by a 5G NR-U BS at the surrounding Wi-Fi devices under co-channel operation in the 6 GHz band. However, maximal performance gains require very narrow beam widths of only several degrees, which may be more achievable in frequency bands above 6 GHz. Furthermore, improvements over using an omnidirectional antenna diminish quickly in dense deployment scenarios. This can be counteracted to a degree by reducing the ratio of 5G NR-U UE to Wi-Fi devices. However, the interference threshold of -91 dBm for bandwidths of 20 MHz and -75 dBm for bandwidths of 320 MHz is only cleared by a large fraction of Wi-Fi devices. In all scenarios except indoor-only Wi-Fi deployments, there are devices left that do not clear the respective threshold, which need to be addressed by an additional interference control mechanism.

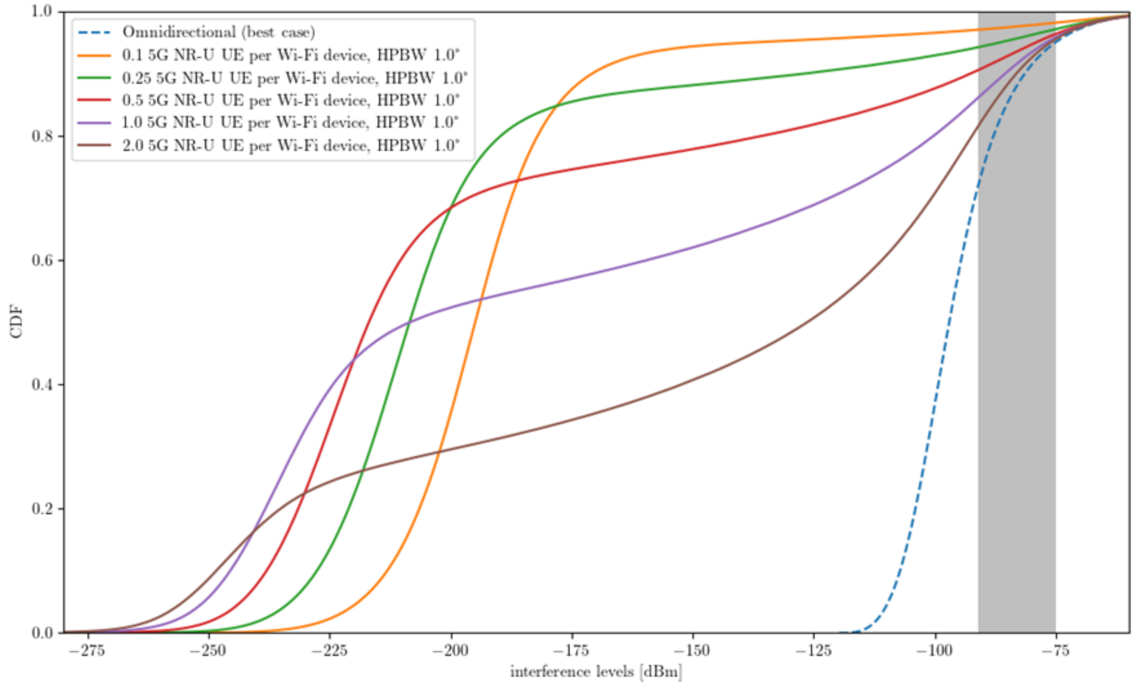

Figure 4-20 Cumulative distribution function of the interference levels at the Wi-Fi devices deployed with a density of 500 Wi-Fi devices/km2 using gaussian beams with a beam width of 1° compared to the distribution of an omnidirectional antenna in an outdoor-only scenario, varying the ratio of simulated 5G NR-U UE to Wi-Fi devices

5 Integration Strategies and Future Regulation Adoption of Advanced Spectrum Management

This section explores pathways for translating the simulation findings and interference mitigation techniques into practical network implementations and regulatory frameworks for future 6G systems. The integration strategy centres on the O-RAN architecture, particularly the RIC framework, which can implement DSS policies through standardized E2 service models and enable real-time coordination between LTE, 5G-NR, and sensing functions. The discussion also addresses how advanced spectrum management techniques – including context-aware interference assessment, dynamic exclusion zones, and adaptive beamforming – can inform the evolution of regulatory policies beyond traditional worst-case static allocation methods toward more flexible, data-driven spectrum governance suitable for ISAC systems operating in shared bands.

5.1 Integration Concept of Advanced Spectrum Management into the RAN-Controller

The O-RAN design methodology establishes the RIC as the central cognitive unit of the mobile network. Acting like a brain of the system, the control applications (e.g., i/x/rApp) on top of the RIC dictate control logic down to the physical layers through the standardized E2 interface.

At the highest level of this architecture resides the Service Management and Orchestration (SMO) framework, which acts as the overarching management layer. Within the SMO, the Non-Real-Time (Non-RT) RIC operates rApps, which function as policy applications. These rApps are responsible for translating high-level operator intent into actionable control policies, which are then transmitted down to the Near Real-Time (Near-RT) RIC via the A1 interface. Additionally, SMO enables automated deployment, reconfiguration, and network observation of the mobile network.

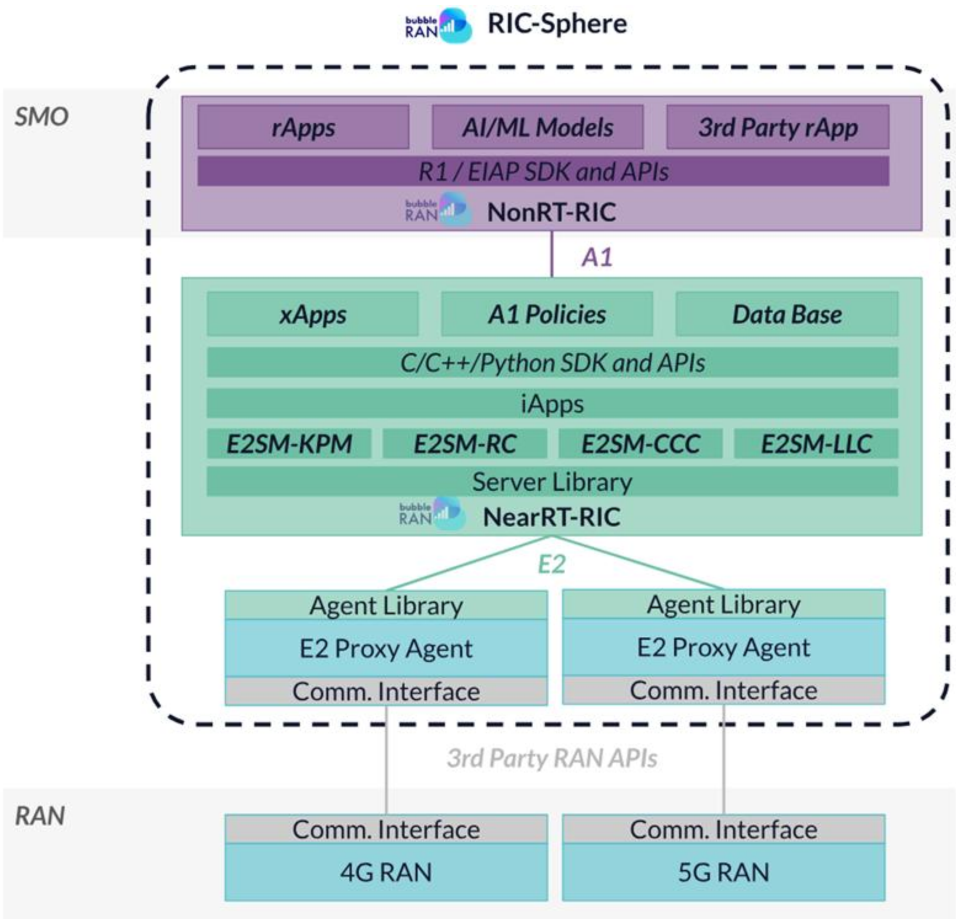

Figure 5-1 Design overview of the RIC Sphere

To advance the Near-RT RIC framework, BubbleRAN introduces the RIC-Sphere [16], a proprietary, modular solution engineered to facilitate seamless integration with third-party equipment vendors, such as OpenAirInterface (OAI), srsRAN/OCUDU and Amarisoft. A defining feature of the MX-RIC ecosystem is its versatile Proxy Agent, which handles a wide array of input/output protocols, including WebSockets, HTTPS, and file-based exchanges.

Architecturally, the system is designed with specific operational mappings:

- **Vendor Integration:** The Proxy Agent maintains a one-to-one relationship with third-party vendor components.
- **Internal Scaling:** The Proxy Agent supports a one-to-many relationship with MX-RIC instances.
- **Developer Extensibility:** The platform functions as a Software Development Kit (SDK), empowering developers to implement custom communication interfaces tailored to specific BS endpoints.

Crucially, both the MX-RIC and the Proxy Agent maintain strict compliance with the O-RAN standardized E2 interface. The system executes standard E2 Application Protocol (E2AP) procedures, seamlessly managing setup, control, and network monitoring functionalities. Underpinning these procedures are the E2 Service Models (E2SM), which utilize standard data structures to provide operational parameters and configuration telemetry.

RIC-Sphere architecture currently provides comprehensive, native support for the following core service models:

- **E2SM-KPM:** Key Performance Monitoring
- **E2SM-RC:** Radio Control
- **E2SM-CCC:** Cell Configuration Control
- **E2SM-LLC:** Low Layer Control

By bridging the Non-RT and Near-RT domains, this architecture directly supports a variety of use cases. Based on current requirements, the operational intent is defined as follows: the policy is co-primary shared access with spectrum pooling, implemented through a composite spectrum scheduler and a dynamic user-based spectrum allocation policy, with Round Robin scheduling at the RAT level. Once the rApp translates this policy and pushes it via the A1 interface, the Near-RT RIC applies the appropriate iApp. These iApps continuously evaluate network conditions and subsequently send targeted control or report services through the E2 service models to enforce the defined spectrum scheduling and allocation behaviors.

5.1.1 Positioning 4G/5G Spectrum Sharing Use Cases

The primary focus is establishing spectrum sharing based on co-primary shared access between the LTE RAT and the 5G-NR RAT. To achieve this, the architecture employs a dynamic user parameter designed specifically for a composite spectrum scheduler.

This approach closely aligns with the network footprint and specific requirements detailed in the official O-RAN specification, specifically [17].

To successfully implement this spectrum sharing model, the O-RAN architecture must meet the following core requirements:

- **Policy Adaptation:** Enable the operator to adapt radio resource allocation policies and control mechanisms to dynamically share radio spectrum between 4G and 5G networks.
- **Resource Control:** Conduct comprehensive resource management and control functions across both RATs.
- **DSS Augmentation:** Release the solution as a DSS application intended to augment the L3, L2, and L1 control functions, utilizing a suitable service model that allows for dynamic modification.

5.1.2 Proposed implementation strategy

Based on the architectural figures and guidelines provided in [17], the proposed implementation strategy is divided into policy translation and active control:

- **Policy Translation via rApps:** An rApp hosted in the non-RT RIC is responsible for translating global DSS policies based on real-time workload requirements. This translation directly informs the composite spectrum scheduler and the dynamic user-based spectrum allocation policy.
- **Control Decisions via iApps:** Based on the resource policies handed down via the A1 interface, the Near-RT RIC applies suitable iApps. These iApps are responsible for executing data collection and making subsequent active control decisions, such as finalizing resource sharing allocations between the LTE and NR nodes.
- **Data Collection Requirements:** To ensure the iApps have the necessary telemetry to make accurate sharing decisions, the system must gather specific network metrics. The detailed parameters required for this data collection phase are outlined in *Table 4.11.4-1: Required data for DSS use case* within [17].

From the perspective of the edge devices evaluated in Section 4, robust RD extraction and interference filtering can be performed locally on COTS devices and localized sensing telemetry can be processed independently from the primary communication link. This pre-processed, high-level sensing data can then be selectively fed to the RAN controller using the xApp interface, minimizing signalling overhead while informing broader network spectrum management decisions.

5.2 Adoption of Advanced Spectrum Management into Future Regulatory Policies

Co-existence questions and interference scenarios as shown in Section 4 as well as appropriate sharing and mitigation scenarios are currently a hot topic in both regulation and standardisation. The results from 6G SENSES on geolocated Wi-Fi exclusions zones [5] have been presented at the IEEE 802 Plenary meeting in Bangkok in November 2025 to all three relevant groups working on this topic, namely IEEE 802.18 TAG Regulation [18], IEEE 802.19 WG Coexistence and IEEE 802.11 SC Coexistence showing high interest in this topic and providing feedback for further investigations.

The implementation of methods like the above-mentioned exclusion zones can be achieved only by flexible spectrum management techniques requiring a paradigm shift in spectrum regulation, where the current static and mostly exclusive spectrum allocation is replaced by dynamic spectrum allocation methods. The interest in this topic is reflected by various documents published by regulatory bodies. In the following a non-exhausting lists the findings from recently published documents are summarized:

- In [2] ITU-R emphasizes, that regulators should recognize the need for flexible frameworks that foster the deployment of spectrum for new applications pointing also to different industry solutions. ITU-R recommends to start the corresponding consultation processes in order to review how spectrum assignment regulations can be implemented. This opens opportunities for industry to demonstrate that interference or sharing issues can be addressed.
- In November 2025 ACMA has published a discussion paper on “Automatic Frequency Coordination-assisted spectrum sharing in the 6 GHz band” [19] asking various stakeholders for comments. In the discussion paper AFC is proposed by using cloud-based databases, geolocation reporting and propagation modelling.
- In January 2026, the UK regulator Ofcom has published a consultation on the process and conditions to enable AFC in the 5925 - 7125 MHz band [20]. One key technical condition identified by Ofcom is the use of a geolocation capability, where ab AFC system shall be accessed in order to determine the

available frequencies and associated maximum transmit power levels at their location prior to transmission.

- Also in January 2026, Ofcom has published another consultation [21], which proposes to implement prioritised spectrum sharing in the Upper 6 GHz band, with
    - A “Wi-Fi- priority” portion in the bottom 160 MHz of the band (6425–6585 MHz),
    - A “mobile priority” portion in the upper 540 MHz (6585–7125 MHz),

  and the possibility to use Wi-Fi in the whole 6 GHz band provided that Wi-Fi is under AFC control, see Figure 5-2.

Current regulatory activities make it probable, that interference mitigation methods as investigated by 6G SENSES, may become reality by the implementation of AFC methods.

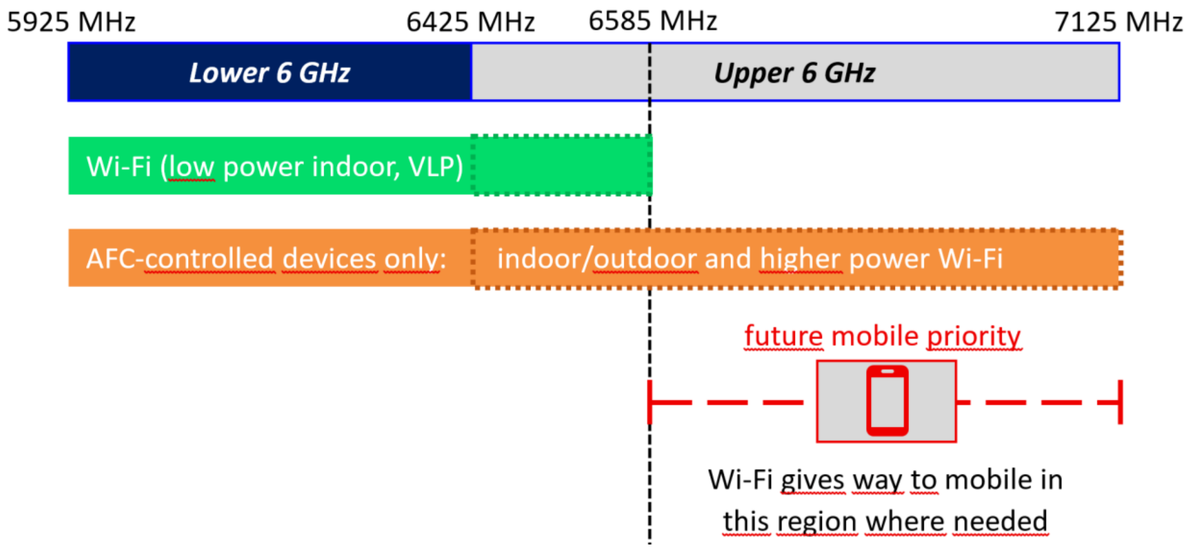

Figure 5-2 Spectrum use as proposed by Ofcom, based on [21].

6 Summary and Conclusions

This deliverable examines advanced spectrum management techniques for three representative interference scenarios of high relevance to emerging 6G systems, namely: cooperative ISAC operation using monostatic Wi-Fi sensing, competitive spectrum sharing between LTE and 5G-NR, and coexistence between 5G NR-U and Wi-Fi in the 6 GHz band. Across these scenarios, measurements and simulations are combined to quantify interference effects and to assess concrete mitigation strategies at the levels of signal processing, radio resource management, and spatial interference control.

For the cooperative ISAC scenario, the results confirm that high-resolution RD processing is a key enabler for robust Wi-Fi-based sensing in interference-rich public environments. Range filtering on RD maps, supported by the coherent processing gain of wideband 6 GHz operation, effectively suppresses background motion and non-cooperative Wi-Fi activity, enabling a temporal CNN-GRU model to maintain gesture recognition accuracy above 90% in a crowded café setting. This demonstrates that interference-aware sensing pipelines can coexist with regular WLAN traffic on COTS hardware without NIC modifications, provided that spatial information is explicitly exploited in the processing chain.

In the LTE/5G-NR spectrum-sharing scenario, it is shown that co-primary shared access with spectrum pooling, coordinated by a composite spectrum scheduler, can provide a flexible migration path from LTE to 5G while maintaining acceptable performance for both RATs. At the same time, the simulations highlight that mixed-numerology operation introduces non-negligible INI, which results in a persistent capacity loss compared to same-numerology configurations for both full-buffer and constant-rate traffic models. These findings indicate that advanced scheduling strategies in multi-RAT deployments must be numerology-aware and explicitly interference-conscious, if dynamic spectrum sharing is to deliver its intended efficiency gains.

For coexistence between 5G NR-U and Wi-Fi in the 6 GHz band, the Monte Carlo simulations underline that purely spatial measures such as static exclusion zones are effective only under specific deployment conditions. Moderate exclusion zone radii can ensure protection of both NR-U BSs and Wi-Fi devices where Wi-Fi deployments are predominantly indoor and benefit from building entry and indoor losses. In contrast, dense outdoor Wi-Fi deployments require very large exclusion radii, on the order of several hundred m, to comply with ITU-R interference criteria, which would significantly reduce usable spectrum and are therefore not viable as a stand-alone measure.

The evaluation of advanced beamforming concepts at the 5G NR-U BS indicates that spatial signal processing can partially mitigate these coexistence challenges. MVDR beamforming with adaptive null placement is able to reduce aggregate interference from surrounding Wi-Fi devices by up to 7-13 dB in low- to medium-density scenarios and maintains an advantage over omnidirectional antennas for indoor-only deployments even at higher densities. Likewise, tracking individual NR-U UEs with narrow Gaussian beams consistently lowers interference at Wi-Fi receivers compared to omnidirectional transmission, although the performance gains diminish as deployment density increases and become significant primarily for narrow beam widths in the order of a few degrees. Overall, the results suggest that spatial techniques are an important element of the interference-management toolkit, but they cannot fully resolve coexistence issues in dense, outdoor-dominated deployments on their own.

On the basis of these technical results, Section 5 outlines how advanced spectrum management concepts can be integrated into an O-RAN-based architecture via the RIC and its rApps/xApps, thereby enabling closed-loop control over numerology selection, spectrum partitioning, beam and null configuration, and potentially exclusion-zone parameters. From a regulatory perspective, current ongoing consultations on AFC methods will likely lead to have these solutions implemented in future deployments.

In summary, the deliverable shows that a combination of signal-level interference suppression, intelligent spectrum-sharing policies, and spatial interference control can substantially increase the flexibility and efficiency of spectrum use in 6G-class networks. At the same time, the strong dependence of performance on deployment density, traffic characteristics, and the indoor/outdoor mix indicates that no single mechanism is sufficient across all cases, and that hybrid strategies orchestrated by a programmable RAN controller is required.

7 References

[1] International Telecommunication Union, "Report ITU-R SM.2093-3 - Guidance on the regulatory framework for national spectrum management," 2018.

[2] Digital Regulation Platform, "Spectrum management: Key applications and regulatory considerations driving the future use of spectrum," 25 04 2025. [Online]. Available: https://digitalregulation.org/spectrum-management-key-applications-and-regulatory-considerations-driving-the-future-use-of-spectrum-2/. [Accessed 24 02 2026].

[3] Federal Communications Commission, "3.5 GHz Band Overview," 03 04 2023. [Online]. Available: https://www.fcc.gov/wireless/bureau-divisions/mobility-division/35-ghz-band/35-ghz-band-overview. [Accessed 24 02 2026].

[4] Digital Regulation Platform, "Spectrum licensing: local and private networks," 20 04 2025. [Online]. Available: https://digitalregulation.org/spectrum-licensing-local-and-private-networks/. [Accessed 24 02 2026].

[5] B. K. Jung and T. Kürner, "Impact of Exclusion Zone on Interference Between 5G NR-U and Wi-Fi Under Co-Channel Operation in the 6 GHz Band," in *2025 IEEE 36th International Symposium on Personal, Indoor and Mobile Radio Communications (PIMRC)*, Istanbul, Turkiye, 2025.

[6] Y.-H. Liu, C.-P. Ku and T.-D. Chiueh, "Design and Implementation of a 5G NR Transmitter With Wi-Fi Coexistence by Beamforming and Power Control," *IEEE Open Journal of the Communications Society,* no. 5, pp. 2132 - 2144, 2024.

[7] P. F. Goldsmith, "Gaussian Beam Propagation," in *Quasioptical Systems: Gaussian Beam Quasioptical Propogation and Applications*, 1998, pp. 9-38.

[8] 3rd Generation Partnership Project (3GPP), "Study on channel model for frequencies from 0.5 to 100 GHz - Technical Report TR 38.901 V16.1.0," 2020.

[9] International Telecommunication Union (ITU), "ITU-R P.2108-1 - Prediction of Clutter Loss," 2021.

[10] International Telecommunication Union (ITU), "ITU-R M.2481-0 - In-band and adjacent band coexistence and compatibility studies between IMT systems in 3300-3400 MHz and radiolocation systems in 3100-3400 MHz," 2019.

[11] International Telecommunication Union (ITU), "ITU-R F.1336-5 - Reference radiation patterns of omnidirectional, sectoral and other antennas for the fixed and mobile services for use in sharing studies in the frequency range from 400 MHz to about 70 GHz," 2019.

[12] International Telecommunication Union (ITU), "ITU-R S.2367-0 - Sharing and compatibility between International Mobile Telecommunication systems and fixed-satellite service networks in the 5850-6425 MHz frequency range," 2015.

[13] European Telecommunications Standards Institute (ETSI), "ETSI EN 303 687 V1.1.1 (2022-08): 6 GHz WAS/RLAN; Harmonized Standard for access to radio spectrum," 2022.

[14] International Telecommunication Union (ITU), „ITU-R S.2367-0 - Sharing and compatibility between International Mobile Telecommunication systems and fixed-satellite service networks in the 5850-6425 MHz frequency range," 2015.

[15] Institute of Electrical and Electronics Engineers (IEEE), "IEEE Std 802.11ax-2021 (Amendment to IEEE Std 802.11-2020): IEEE standard for information technology–telecommunications and information

exchange between systems local and metropolitan area networks–specific requirements part 11," 2021.

[16] BubbleRAN, "RIC-Sphere: BubbleRAN RAN Intelligent Controller DataSheet," BubbleRAN, 01 2026. [Online]. Available: https://bubbleran.com/resources/files/BubbleRAN-RIC-Sphere-Datasheet.pdf. [Accessed 13 03 2026].

[17] European Telecommunications Standards Institute (ETSI), "Publicly Available Specification (PAS); O-RAN Use Cases Detailed Specification; (O-RAN.WG1.Use-Cases-Detailed-Specification-R003-v12.00)," 2025.

[18] B. K. Jung and T. Kürner, "Impact of Exclusion Zone on Interference Between 5G NR-U and Wi-Fi under Co-Channel Operation in the 6 GHz Band," 11 2025. [Online]. Available: https://mentor.ieee.org/802.18/dcn/25/18-25-0107-00-0000-impact-of-exclusion-zone-on-interference-between-5g-nr-u-and-wi-fi-under-co-channel-operation-in-the-6-ghz-band.pdf. [Accessed 25 03 2026].

[19] Australian Communications and Media Authority (ACMA), "Automatic Frequency Coordination-assisted spectrum sharing in the 6 GHz band," 11 2025. [Online]. Available: https://www.acma.gov.au/sites/default/files/2025-10/Discussion%20paper_Automatic%20Frequency%20Coordination-assisted%20spectrum%20sharing%20in%20the%206%20GHz%20band.pdf. [Accessed 25 03 2026].

[20] UK OFCOM, "Consultation: Enabling automated frequency coordination (AFC) in the 6 GHz band," 2026. [Online]. Available: https://www.ofcom.org.uk/spectrum/innovative-use-of-spectrum/enabling-automated-frequency-coordination-afc-in-the-6-ghz-band. [Accessed 25 03 2026].

[21] UK OFCOM, "Consultation: Expanding access to the 6 GHz band for commercial mobile and Wi-Fi services - Next steps for Wi-Fi," 2026. [Online]. Available: https://www.ofcom.org.uk/siteassets/resources/documents/consultations/category-3-4-weeks/consultation-expanding-access-to-the-6-ghz-band-for-commercial-mobile-and-wi-fi-services/main-document/expanding-access-to-the-6-ghz-band-for-commercial-mobile-and-wi. [Accessed 25 03 2026].

8 Acronyms

Acronym	Description
3GPP	3rd Generation Partnership Project
4G	Fourth generation mobile network
5G	Fifth generation mobile network
5G NR	5G New Radio
5G NR-U	5G NR Unlicensed
6G	Sixth generation mobile network
ACMA	Australian Communications and Media Authority
AFC	Automated Frequency Coordination
AP	Access Point
APT	Asia-Pacific Telecommunity
BNetzA	Bundesnetzagentur (German Federal Network Agency)
BR	BubbleRAN
BS	Base Station
CBRS	Citizens Broadband Radio Service
CDF	Cumulative Distribution Function
CEPT	Conference of Postal and Telecommunications Administrations
CF-mMIMO	Cell-Free Massive Multiple Input Multiple Output
CITEL	Inter-American Telecommunication Commission
COTS	Commercial Off-The-Shelf
DSS	Dynamic Spectrum Sharing
EMC	Electromagnetic Compatibility
ETSI	European Telecommunications Standards Institute
FCC	Federal Communications Commission
GAA	General Authorized Access
HPBW	Half-Power Beam Width
HAPS	High-Altitude Platform Station
IEEE	Institute of Electrical and Electronics Engineers
IMT	International Mobile Telecommunications
INI	Inter-Numerology Interference
IHP	Leibniz-Institut für innovative Mikroelektronik
INT	Intel
IoT	Internet of Things

ISAC	Integrated Sensing and Communication
ISD	Inter-Site Distance
ITU	International Telecommunication Union
ITU-R	International Telecommunication Union – Radiocommunication Sector
LO	Local Oscillator
LTE	Long Term Evolution
MIFR	Master International Frequency Register
MIMO	Multiple Input Multiple Output
ML	Machine Learning
MNO	Mobile Network Operator
MVDR	Minimum-variance distortionless response
NGSO	Non-Geostationary Satellite Orbit
NIC	Network Interface Card
NTU	Nottingham Trent University
OAI	Open Air Interface
Ofcom	Office of Communications
O-RAN	Open Radio Access Network
OFDM	Orthogonal Frequency Division Multiplexing
OTE	Hellenic Telecommunications Organization
PAL	Priority Access License
QoS	Quality of Service
R&D	Research and Development
RAN	Radio Access Network
RAT	Radio Access Technology
RB	Resource Block
RD	Range-Doppler
RIC	RAN Intelligent Controller
RIS	Reconfigurable Intelligent Surface
RR	Radio Regulations
SAS	Spectrum Access System
SiMoNe	Simulator for Mobile Networks
SMO	Service Management and Orchestration
SNR	Signal-to-Noise Ratio
SNS JU	Smart Networks and Services Joint Undertaking
ToC	Table of Contents

TTI	Transmission Time Interval
TUBS	Technische Universität Braunschweig
U-NII-7	Unlicensed National Information Infrastructure band 7
UE	User Equipment
UK	United Kingdom
ULA	Uniform Linear Array
Wi-Fi	Wireless Fidelity
WLAN	Wireless Local Area Network
WRC	World Radiocommunication Conference